

anQCD: a *Mathematica* package for calculations in general analytic QCD models

César Ayala^a, Gorazd Cvetič^a

^a*Department of Physics, Universidad Técnica Federico Santa María,
Casilla 110-V, Valparaíso, Chile*

Abstract

We provide a *Mathematica* package that evaluates the QCD analytic couplings (in the complex domain) $\mathcal{A}_\nu(Q^2)$, which are analytic analogs of the powers $a(Q^2)^\nu$ of the underlying perturbative QCD (pQCD) coupling $a(Q^2) \equiv \alpha_s(Q^2)/\pi$, in three analytic QCD models (anQCD): Fractional Analytic Perturbation Theory (FAPT), Two-delta analytic QCD (2 δ anQCD), and Massive Perturbation Theory (MPT). The analytic (holomorphic) running couplings $\mathcal{A}_\nu(Q^2)$, in contrast to the corresponding pQCD expressions $a(Q^2)^\nu$, reflect correctly the analytic properties of the spacelike observables $\mathcal{D}(Q^2)$ in the complex Q^2 plane as dictated by the general principles of quantum field theory. They are thus more suited for evaluations of such physical quantities, especially at low momenta $|Q^2| \sim 1 \text{ GeV}^2$.

PACS numbers: 12.38.Bx, 11.15.Bt, 11.10.Hi, 11.55.Fv

Program Summary

Title of program: anQCD

The main program (anQCD.m) and supplementary modules (Li_nu.m and s0r.m), and the zipped file containing all three files (anQCD_Mathematica.zip), available from the web page:

gcvetic.usm.cl

Computer for which the program is designed and others on which it is operable: Any work-station or PC where **Mathematica** is running.

Operating system or monitor under which the program has been tested: Operating system Linux and Mac OS X, software Mathematica 9.0.1, 10.0.1 and 10.0.2

No. of bytes in distributed program including test data etc.:

63 kB (main module anQCD.m), 2 kB (supplementary module Li_nu.m), 18 kB (supplementary module s0r.m);

Distribution format: ASCII

Keywords: Analyticity, Fractional Analytic Perturbation Theory, Two-delta analytic QCD model, Massive Perturbation Theory, Perturbative QCD, Renormalization group evolution.

Nature of the physical problem: Evaluation of the values for analytic couplings $\mathcal{A}_\nu(Q^2; N_f)$ in analytic QCD [the analytic analog of the power $(\alpha_s(Q^2; N_f)/\pi)^\nu$] based on the dispersion relation; \mathcal{A}_ν represents a physical (holomorphic) function in the plane of complex squared momenta $-q^2 \equiv Q^2$. In anQCD.m we collect the formulas for three different analytic models depending on the energy scale, Q^2 , number of flavors N_f , the QCD scale $\bar{\Lambda}_{N_f}$, and the (nonpower) index ν . The considered models are: Analytic Perturbation theory (APT), Two-delta analytic QCD (2 δ anQCD) and Massive Perturbation Theory (MPT).

Method of solution: anQCD uses **Mathematica** functions to perform numerical integration of spectral function for each analytic model, in order to obtain the corresponding analytic images $\mathcal{A}_\nu(Q^2)$ via dispersion relation.

Restrictions on the complexity of the problem: It could be that for an unphysical choice of the input parameters the results are meaningless.

Typical running time: For all operations the running time does not exceed a few seconds.

1. Introduction

The perturbative approach to QCD (pQCD) works well for evaluations of physical quantities at high momentum transfer ($|q^2| \gtrsim 10^1 \text{ GeV}^2$). However, it is unreliable at low momenta ($|q^2| \sim 1 \text{ GeV}^2$), the principal reason for this being the existence of singularities of the pQCD coupling parameter $a(Q^2) \equiv \alpha_s(Q^2)/\pi$ (where $Q^2 \equiv -q^2$) at such complex spacelike momenta Q^2 : $|Q^2| \lesssim 1 \text{ GeV}^2$ and $Q^2 \not\leq 0$. These (Landau) singularities reappear in evaluations of the spacelike observables $\mathcal{D}(Q^2)$ for small $|Q^2|$. For example, if $\mathcal{D}(Q^2)$ is dominated by the leading-twist term of dimension zero, its evaluated expression is $f(a(\kappa Q^2))$ where f is a (truncated) power series in $a(\kappa Q^2)$ and the positive κ (~ 1) is the renormalization scale parameter. Hence $f(a(\kappa Q^2))$ has the same region of singularities as $a(\kappa Q^2)$. This does not reflect correctly the true analyticity structure of the spacelike observable $\mathcal{D}(Q^2)$. Such an observable must be, by the general principles of the local quantum field theory [1, 2], a holomorphic (analytic) function in the complex Q^2 plane except on parts of the negative semiaxis where it has a cut; i.e., analyticity for $Q^2 \in \mathbb{C} \setminus (-\infty, 0]$. Therefore, the coupling parameter $\mathcal{A}_1(Q^2)$, that is to be used instead of $a(Q^2)$ to evaluate the spacelike observables $\mathcal{D}(Q^2)$, should have qualitatively the same analyticity properties, i.e., $\mathcal{A}_1(Q^2)$ should be a holomorphic function for $Q^2 \in \mathbb{C} \setminus (-\infty, 0]$. Such an analytic function $\mathcal{A}_1(Q^2)$ defines what is called analytic QCD (anQCD) model.

The finiteness of the QCD coupling in the infrared regime and, in general, the holomorphic behavior of it in the Q^2 complex plane, are suggested by various independent lines of research in QCD, among them: by the Gribov-Zwanziger approach [3]; by analyses of Dyson-Schwinger equations in QCD [4, 5] and by other functional methods [6, 7]; by lattice calculations [8]; by models using the AdS/CFT correspondence modified by a dilaton background [9]; in various other approaches such as those in Refs. [10–15].

The first anQCD model, constructed explicitly in the aforementioned sense, is the Analytic Perturbation Theory (APT) of Shirkov, Solovtsov *et al.* [16–19]. The underlying pQCD discontinuity function $\rho_1^{(\text{pt})}(\sigma) \equiv \text{Im}a(Q^2 = -\sigma - i\epsilon)$ was kept unchanged on the entire negative axis in the Q^2 -plane, i.e., $\text{Im}\mathcal{A}_1^{(\text{APT})}(-\sigma - i\epsilon) = \rho_1^{(\text{pt})}(\sigma)$ for all $\sigma \geq 0$. On the other hand, the Landau discontinuity region (at $-\Lambda_{\text{Lan.}}^2 \leq \sigma < 0$) was eliminated, i.e., $\text{Im}\mathcal{A}_1^{(\text{APT})}(-\sigma - i\epsilon) = 0$ for $\sigma < 0$. The resulting coupling $\mathcal{A}_1^{(\text{APT})}(Q^2)$ for $Q^2 \in \mathbb{C} \setminus (-\infty, 0]$ was then obtained by the use of a dispersion relation involving $\rho_1^{(\text{pt})}(\sigma)$ at $\sigma \geq 0$. The analogs $\mathcal{A}_n^{(\text{APT})}(Q^2)$ of integer powers $a(Q^2)^n$ were also constructed in the aforementioned works. An extension to the analogs $\mathcal{A}_\nu^{(\text{APT})}(Q^2)$ of noninteger powers $a(Q^2)^\nu$ in this model were obtained and used in the works [20–23]; hence this anQCD model is also called Fractional APT (FAPT).

Later on, other analytic QCD models were constructed, which fulfill certain additional physically motivated restrictions, such as Refs. [24–32]. Analytic QCD models, as well as related dispersive approaches, have been used in evaluations of various low-momentum QCD quantities, cf. Refs. [33–39]. Reviews of the analytic QCD approaches are given in Refs. [40–45].

In addition to FAPT, we will consider here the Two-delta analytic QCD ($2\delta\text{anQCD}$) [31] and Massive Perturbation Theory (MPT) [32]. The $2\delta\text{anQCD}$ model [31]

is similar to FAPT model in the sense that it is (partially) based on the underlying pQCD coupling $a(Q^2)$: $\text{Im}\mathcal{A}_1^{(2\delta)}(-\sigma - i\epsilon) = \rho_1^{(\text{pt})}(\sigma)$ for large enough $\sigma \geq M_0^2$ (where $M_0 \sim 1$ GeV is a ‘‘pQCD-onset’’ scale). On the other hand, in the (otherwise unknown) low- σ regime, $0 < \sigma < M_0^2$, the behavior of the discontinuity function $\rho_1(\sigma) \equiv \text{Im}\mathcal{A}_1^{(2\delta)}(Q^2 = -\sigma - i\epsilon)$ is parametrized by two positive delta functions. The coupling $\mathcal{A}_1^{(2\delta)}(Q^2)$ is then obtained by the use of a dispersion relation involving $\rho_1(\sigma)$. The parameters for the delta functions and M_0 are determined by requiring that the model effectively merges with the pQCD for large $|Q^2| > \Lambda^2$ (where $\Lambda^2 \sim 0.1$ GeV²), and by requiring that the model reproduce the experimentally determined value $r_\tau = 0.203$ of the τ lepton semihadronic nonstrange $V + A$ decay rate ratio. On the other hand, Massive Perturbation Theory (MPT) [32] is defined via the identity $\mathcal{A}_1(Q^2) = a(Q^2 + m_{\text{gl}}^2)$, where $m_{\text{gl}} \sim 1$ GeV is an effective dynamical gluon mass.

In general anQCD models, such as $2\delta\text{anQCD}$ or MPT, the formalism for construction of analytic analogs $\mathcal{A}_\nu(Q^2)$ of the powers $a(Q^2)^\nu$ was formulated in Refs. [27, 28] for the case of integer index ν , and in Ref. [46] for general (noninteger) index ν . Generally we have $\mathcal{A}_\nu \neq (\mathcal{A}_1)^\nu$.

Presently, there exist programs for numerical evaluation of the APT and ‘‘massive’’ APT (MAPT) [47], and of FAPT couplings [48]. The purpose of this work is to offer an extended program in `Mathematica` which numerically evaluates the couplings in FAPT, $2\delta\text{anQCD}$ and in MPT, in order to correctly evaluate (truncated) perturbation series of physical quantities in these anQCD models. Our program evaluates the FAPT couplings in a similar way as the program of Ref. [48]; but the part of our program which evaluates the $2\delta\text{anQCD}$ and MPT couplings is new.

We summarize in Sec. 2 the calculation of the running coupling of the underlying pQCD, the threshold matching, and the corresponding QCD scales $\bar{\Lambda}_{N_f}$. In Sec. 3 we present a general method for calculation of the analytic analogs $\mathcal{A}_\nu(Q^2)$ of powers $a(Q^2)^\nu$ in anQCD models, and a description of the three mentioned anQCD models: FAPT, $2\delta\text{anQCD}$ (with new extension for $N_f \geq 4$), and MPT. In addition, curves of some of the resulting couplings as a function of Q^2 , at positive Q^2 , are presented. Finally, in Sec. 4 we present some practical aspects and the main procedures of the calculational program, as well as some specific examples. More detailed definitions of the procedures are included in Appendix A.

2. Running coupling in the underlying perturbative QCD

2.1. Running coupling at fixed N_f

The differential equation that defines the beta function and therefore the running coupling in perturbative QCD (pQCD) is given by the renormalization group equation (RGE, at renormalization scale $\mu^2 = Q^2$)

$$\beta(a(Q^2)) = Q^2 \frac{\partial a(Q^2)}{\partial Q^2} = - \sum_{j=2}^{\infty} \beta_{j-2}(N_f) a^j(Q^2), \quad (1)$$

with the notation: $a(Q^2) \equiv \alpha_s(Q^2)/\pi = g_s(Q^2)^2/(4\pi^2)$ and N_f is the number of active quarks flavors. The first two beta coefficients (β_0 and β_1 , [49, 50]) are scheme independent, i.e., they are universal in the mass independent renormalization schemes

$$\beta_0(N_f) = \frac{1}{4} \left(11 - \frac{2}{3} N_f \right), \quad \beta_1(N_f) = \frac{1}{16} \left(102 - \frac{38}{3} N_f \right). \quad (2)$$

The next coefficients (β_2, β_3, \dots) are scheme dependent; in fact, they define the renormalization scheme [51]. In the $\overline{\text{MS}}$ scheme, β_2 and β_3 are known [52, 53]

$$\bar{\beta}_2(N_f) = \frac{1}{64} \left(\frac{2857}{2} - \frac{5033}{18} N_f + \frac{325}{54} N_f^2 \right), \quad (3a)$$

$$\begin{aligned} \bar{\beta}_3(N_f) = & \frac{1}{256} \left[\left(\frac{149753}{6} + 3564\zeta_3 \right) - \left(\frac{1078361}{162} + \frac{6508}{27}\zeta_3 \right) N_f \right. \\ & \left. + \left(\frac{50065}{162} + \frac{6472}{81}\zeta_3 \right) N_f^2 + \frac{1093}{729} N_f^3 \right] \end{aligned} \quad (3b)$$

where ζ_ν is the Riemann zeta function, in particular $\zeta_3 \simeq 1.202057$.

The beta function on the right-hand side of Eq. (1) is usually approximated as a truncated perturbation series of coupling a . The resulting differential equation for a is solved, either analytically (if possible) or numerically. For example, the one-loop order equation can be integrated explicitly, giving the well known solution

$$a(Q^2) = \frac{1}{\beta_0 \ln(Q^2/\bar{\Lambda}^2)}, \quad \bar{\Lambda}^2 = \mu^2 e^{-1/(\beta_0 a(\mu^2))}. \quad (4)$$

One way to solve the RGE at the two-loop level is to iterate with respect to the one-loop formula. This gives us an approximate coupling as an expansion in powers of L^{-1} , where $L \equiv \ln(Q^2/\bar{\Lambda}^2)$. If we truncate at L^{-2} , we obtain

$$a^{(2,L^2)}(Q^2) = \frac{1}{\beta_0 L} \left(1 - \frac{\beta_1 \ln(L)}{\beta_0^2 L} \right). \quad (5)$$

The iterative method can be performed at any loop level. For example, when truncating the expansion of the M -loop coupling at $L^{-\mathcal{N}} \equiv 1/\ln^{\mathcal{N}}(Q^2/\bar{\Lambda}^2)$, we obtain¹

$$\begin{aligned} a^{(M,L\mathcal{N})}(Q^2) = & \frac{1}{\beta_0 L} \left\{ 1 - \frac{\beta_1 \ln(L)}{\beta_0^2 L} + \frac{1}{\beta_0^2 L^2} \left[\frac{\beta_1^2}{\beta_0^2} (\ln^2(L) - \ln(L) - 1) + \frac{\beta_2}{\beta_0} \right] + \right. \\ & \frac{1}{\beta_0^3 L^3} \left[\frac{\beta_1^3}{\beta_0^3} \left(-\ln^3(L) + \frac{5}{2} \ln^2(L) + 2\ln(L) - \frac{1}{2} \right) - 3 \frac{\beta_1 \beta_2}{\beta_0^2} \ln(L) + \frac{\beta_3}{2\beta_0} \right] + \\ & \left. \frac{1}{\beta_0^{\mathcal{N}-1} L^{\mathcal{N}-1}} \left[\frac{\beta_1^{\mathcal{N}-1}}{\beta_0^{\mathcal{N}-1}} (-1)^{\mathcal{N}-1} \ln^{\mathcal{N}-1} L + \dots \right] \right\}. \end{aligned} \quad (6)$$

¹ The superscript notation $(M, L\mathcal{N})$ in Eq. (6) means that the expansion is truncated at $1/L^{\mathcal{N}}$, and that M -loop β -function is taken, i.e., $\beta_j = 0$ for $j \geq M$. For consistency reasons, we must have $\mathcal{N} \geq M$. In practice, the expansion gives us expression which, for $Q^2 > \bar{\Lambda}^2$, tends toward the exact M -loop coupling $a^{(M)}(Q^2)$ when $\mathcal{N} \rightarrow \infty$ (i.e., $\mathcal{N} \gg M$).

There is a way to find the two-loop coupling as a solution of RGE exactly. The two-loop RGE leads to a transcendental equation. Namely, integrating (1), with $\beta_k = 0$ for ($k = 2, 3, \dots$), we have

$$\int_{a(\mu^2)}^{a(Q^2)} \frac{da}{a^2 \left(1 + \frac{\beta_1}{\beta_0} a\right)} = -\beta_0 \int_0^{\frac{1}{2} \ln(Q^2/\mu^2)} d \ln(Q^2/\mu^2). \quad (7)$$

So, the transcendental equation gets the form

$$\ln(Q^2/\mu^2) = C + \frac{1}{\beta_0 a(Q^2)} + \frac{\beta_1}{\beta_0^2} \ln(a(Q^2)) - \frac{\beta_1}{\beta_0^2} \ln \left(1 + \frac{\beta_1}{\beta_0} a(Q^2)\right), \quad (8)$$

where C contains the coupling $a(\mu^2)$.

A new invariant mass parameter Λ can be introduced, given by

$$\begin{aligned} \ln(Q^2/\Lambda^2) &= \frac{1}{\beta_0 a(Q^2)} - \frac{\beta_1}{\beta_0^2} \ln \left(\frac{\beta_1}{\beta_0^2} + \frac{1}{\beta_0 a(Q^2)} \right), \\ \Lambda^2 &= \mu^2 \exp \left[C - \frac{\beta_1}{\beta_0^2} \ln(\beta_0) \right]. \end{aligned} \quad (9)$$

This relation must be inverted; however, nontrivial problems related to the singularity structure appear. The solution is achieved with the help of the so-called Lambert W function defined by

$$W(z) \exp[W(z)] = z. \quad (10)$$

The singularity structure of the Lambert function consists of an infinite number of branches; it satisfies the following symmetry relation: $W_{-n}^*(y^*) = W_n(y)$.

With this function the solution to the coupling is [34, 54]

$$a^{(2)}(Q^2) = -\frac{1}{c_1} \frac{1}{1 + W_{\mp 1}(z_{\pm})}, \quad (11)$$

where $c_1 = \beta_1/\beta_0$, $Q^2 = |Q^2|e^{i\phi}$, and the upper sign refers to the case $0 \leq \phi \leq +\pi$, the lower sign to $-\pi \leq \phi \leq 0$, and

$$z_{\pm} = \frac{1}{c_1 e} \left(\frac{|Q^2|}{\Lambda^2} \right)^{-\beta_0/c_1} \exp \left[i \left(\pm\pi - \frac{\beta_0}{c_1} \phi \right) \right]. \quad (12)$$

This idea can be extended to the higher loop case, using for the beta function $\beta(a)$ the form of Padé [3/1](a)

$$\beta_{[3/1]}(a) = -\beta_0 a^2(Q^2) \frac{1 + (c_1 - c_2/c_1)a(Q^2)}{1 - (c_2/c_1)a(Q^2)} \quad (13a)$$

$$= -\beta_0 a^2(Q^2) \left[1 + c_1 a(Q^2) + c_2 a(Q^2)^2 + \frac{c_2^2}{c_1} a(Q^2)^2 + \frac{c_2^3}{c_1^2} a(Q^2)^3 + \dots \right], \quad (13b)$$

where the renormalization scheme parameters are: $\beta_2 = \beta_0 c_2$ and $\beta_j = \beta_0 c_2^{j-1} / c_1^{j-2}$ ($j \geq 3$). We call this scheme c_2 -Lambert scheme. When c_2 in the beta function (13) is chosen to be in $\overline{\text{MS}}$ scheme, i.e., $c_2 = \bar{c}_2 (= \bar{\beta}_2 / \beta_0)$, we will refer to this scheme, somewhat loosely, as 3-loop $\overline{\text{MS}}$ in pQCD, FAPT and MPT (the 4-loop coefficient $\beta_3 = \beta_0 \bar{c}_2^2 / c_1$ is not $\overline{\text{MS}}$). With this, the solution of the coupling to three loops in terms of the Lambert function takes the form [55]²

$$a(Q^2) = -\frac{1}{c_1} \frac{1}{1 - c_2/c_1^2 + W_{\mp 1}(z_{\pm})}. \quad (14)$$

The Lambert function $W = W(z)$ is defined via the inverse relation (10), cf. Fig. 1(a).

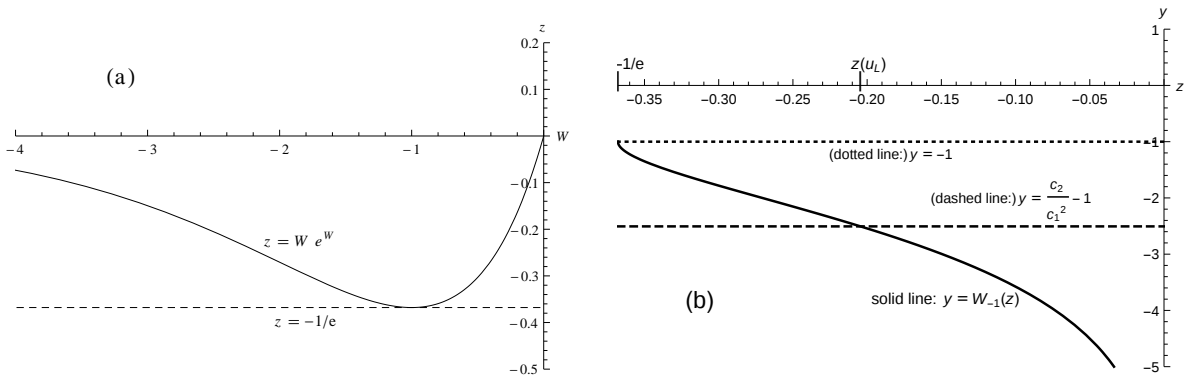


Figure 1: (a) The defining relation $z = W e^W$ for the Lambert function $W(z)$, for $-1/e < z < 0$; (b) The branch $W_{-1}(z)$ for the same z -interval; when $c_2 < 0$, the denominator of Eq. (14) becomes zero at a $z(u_L)$ in this interval.

The two branches $W_{\mp 1}(z)$ of the Lambert function are related via complex-conjugation $W_{+1}(z^*) = W_{-1}(z)^*$, and the point $z = -1/e$ is the branching point of these functions. In the interval $-1/e < z < 0$, $W_{-1}(z)$ is a decreasing function of z , cf. Fig. 1(b). When $z \rightarrow -0$, the scale Q^2 tends to $Q^2 \rightarrow +\infty$, and $W_{-1}(z) \rightarrow -\infty$, this reflecting the asymptotic freedom of $a(Q^2)$ of Eq. (14).

The coupling (14) with the $\overline{\text{MS}}$ value $c_2 = \bar{c}_2(N_f) \equiv \bar{\beta}_2(N_f) / \bar{\beta}_0(N_f)$ will be the underlying pQCD coupling in those analytic models which we call: 3-loop FAPT $_{N_f}$, 3-loop global FAPT,³ and 3-loop MPT $_{N_f}$. In $2\delta\text{anQCD}$, the underlying pQCD coupling will also be that of Eq. (14), but with the scheme parameter c_2 in the interval $-5.6 < c_2 < -2$, cf. Table 2 later (with $c_2 = -4.9$ being the preferred illustrative value).

2.2. Thresholds and global coupling

We note that the dependence on the number of effective quark flavors (N_f) is in the beta coefficients (2)-(3). We use the following notations: the N_f 'th quark flavor has

²In the expression (12), the ‘‘Lambert’’ scale Λ is different from the scale $\bar{\Lambda}$ appearing in the expansion (6). Therefore, as we use the latter as an input, the program relates these two scales by equating Eq. (6) [with: $\beta_j / \beta_0 \equiv c_j = c_2^{j-1} / c_1^{j-2}$ ($j = 2, 3, \dots$), cf. the expansion (13b)] with Eq. (14) at high Q^2 ($\sim 10^{10} \text{GeV}^2$).

³For the details of the definition of the ($\overline{\text{MS}}$) 3-loop global FAPT, see Secs. 2.2 and 3.2.

the $\overline{\text{MS}}$ mass $m_{N_f} \equiv \overline{m}_q \equiv \overline{m}_q(\overline{m}_q)$, where $q = c, b, t$ for $N_f = 4, 5, 6$, respectively (we consider $\overline{m}_u, \overline{m}_d, \overline{m}_s \approx 0$). QCD_{N_f} is applied, in principle, at the scales $\mu \equiv \sqrt{|Q^2|}$ such that $m_{N_f} \ll \mu \ll m_{N_f+1}$; in practice, it is applied at μ 's such that $m_{N_f} \lesssim \mu \lesssim m_{N_f+1}$. If the threshold scale is chosen to be $Q_{\text{thr}}^2 = m_{N_f}^2$, the one-loop quark threshold condition is the continuity of the coupling $a(Q^2)$ there; i.e., at $Q^2 = m_{N_f}^2$ we have for $a(Q^2, \overline{\Lambda}^2, N_f)$

$$a(m_{N_f}^2, \overline{\Lambda}_{N_f-1}^2, N_f - 1) = a(m_{N_f}^2, \overline{\Lambda}_{N_f}^2, N_f) . \quad (15)$$

At a higher loop level, a noncontinuous matching has to be performed between the couplings in the effective theories QCD_{N_f} and QCD_{N_f-1} . If the coupling runs according to the N -loop $\overline{\text{MS}}$ beta function, the $(N - 1)$ -loop matching condition should be used. According to the results of Ref. [56], the 3-loop matching condition (for the case of 4-loop $\overline{\text{MS}}$ RGE running) has the form

$$\begin{aligned} a' &= a - a^2 \frac{\ell_h}{6} + a^3 \left(\frac{\ell_h^2}{36} - \frac{19}{24} \ell_h + \tilde{c}_2 \right) + a^4 \left[-\frac{\ell_h^3}{216} \right. \\ &\quad \left. - \frac{131}{576} \ell_h^2 + \frac{\ell_h}{1728} (-6793 + 281(N_f - 1)) + \tilde{c}_3 \right], \end{aligned} \quad (16)$$

where: $\ell_h = \ln[\mu_{N_f}^2/\overline{m}_q^2]$; $a' = a(\mu_{N_f}^2; N_f - 1)$ and $a = a(\mu_{N_f}^2; N_f)$ in $\overline{\text{MS}}$; and

$$\tilde{c}_2 = \frac{11}{72}, \quad \tilde{c}_3 = -\frac{82043}{27648} \zeta_3 + \frac{564731}{124416} - \frac{2633}{31104} (N_f - 1) . \quad (17)$$

The threshold scale is $\mu^{(N_f)} = \kappa \overline{m}_q$ ($\ell_h = 2 \ln \kappa$), where $q = c, b, t$ for $N_f = 4, 5, 6$, respectively; and usually $1 \leq \kappa \leq 3$ is taken.⁴

In Table 1, we present the results for various scales $\overline{\Lambda}_{N_f}$ in pQCD, for the case of the 4-loop RGE running in $\overline{\text{MS}}$ scheme and the corresponding 3-loop threshold matching with $\kappa = 2$ [thresholds at $Q = \kappa \overline{m}_q$], i.e., the 4/3-loop case; and for the 2-loop RGE running and 1-loop threshold matching with $\kappa = 2$ and $\kappa = 1$, i.e., the 2/1-loop case. For the starting value in the numerical integration of the RGE, we used the present world average value $a(M_Z^2; N_f = 5) = 0.1184/\pi$ [57] in $\overline{\text{MS}}$. In all cases, the values of $\overline{\Lambda}_{N_f}$ were determined by equating the numerically obtained (“exact”) values of $a(Q^2)$ with those of the expansion (6) with $\mathcal{N} = 8$; the matchings for $N_f = 5, 4, 3$ were made at the corresponding positive maximal values of the N_f -range, i.e., at $Q^2 = (\kappa \overline{m}_q)^2$, where $\overline{m}_q = \overline{m}_t, \overline{m}_b, \overline{m}_c$ for $N_f = 5, 4, 3$, respectively. The used values of the $\overline{\text{MS}}$ masses $\overline{m}_q \equiv \overline{m}_q(\overline{m}_q)$ were: 1.27 GeV [57], 4.2 GeV [58], 163 GeV (cf., e.g., [59]), respectively. The value of the scale $\overline{\Lambda}_6$ was determined by equating the expansion (6) with the numerical values $a(Q^2; N_f = 6)$ at large momenta ($Q \gtrsim 10^3$ GeV). The 4/3-loop results change insignificantly when the threshold matching parameter changes from $\kappa = 2$ to $\kappa = 1$: $\overline{\Lambda}_3$

⁴ For the evaluation of $a(Q^2)$ at a complex Q^2 , the N_f value assigned is determined by $(\kappa m_{N_f})^2 < |Q^2| < (\kappa m_{N_f+1})^2$, i.e., with such N_f we have $a(Q^2) = a(Q^2; N_f)$.

Table 1: Comparison between different values of the scales $\overline{\Lambda}_{N_f}$ (in MeV) for various N_f , and the values of the $\overline{\text{MS}}$ coupling \overline{a} at various thresholds: (a) the first line is for the 3-loop threshold matching (16) at thresholds $2\overline{m}_q$ and 4-loop RGE-running in $\overline{\text{MS}}$ scheme ($\overline{\beta}_j = 0$ for $j \geq 4$); (b) the second line is for 1-loop threshold matching at $2\overline{m}_q$ and 2-loop RGE running; (c) as the case (b), but with $\kappa = 1$, i.e., the continuous conditions (15) at thresholds \overline{m}_q . In all cases, the expansions (6) with $\mathcal{N} = 8$, and the world average value $\alpha_s(M_Z^2, \overline{\text{MS}}) = 0.1184$ [57] are used.

Method	$\overline{\Lambda}_{N_f}$				$\overline{a}(N_f)$ ($\overline{a}(N_f - 1)$)		
	Λ_6	Λ_5	Λ_4	Λ_3	$N_f = 6$	$N_f = 5$	$N_f = 4$
4/3-loop, $\kappa = 2$	90.6	213.3	297.0	341.8	0.03187(0.03161)	0.05948(0.05842)	0.08706(0.08446)
2/1-loop, $\kappa = 2$	89.7	216.7	312.6	375.3	0.03185(0.03162)	0.05934(0.05852)	0.08650(0.08477)
2/1-loop, $\kappa = 1$	90.7	216.7	308.1	361.8	0.03465(0.03465)	0.07154(0.07154)	0.12061(0.12061)

value decreases by 1.2 MeV, and $\overline{\Lambda}_4$ value by 0.4 MeV. The 2/1-loop values, however, change significantly when we change $\kappa = 2$ to $\kappa = 1$: $\overline{\Lambda}_3$ decreases from 375.3 to 361.8 MeV; $\overline{\Lambda}_4$ decreases from 312.6 to 308.1 MeV. In all cases (4/3 and 2/1-loop), the value $\overline{\Lambda}_5$ is independent of κ (because the initial value is at $Q^2 = M_Z^2$, i.e., where $N_f = 5$); the value of $\overline{\Lambda}_6$ varies insignificantly in the 4/3-loop case, and in the 2/1-loop case it increases by 1 MeV when κ changes from 2 to 1.

In FAPT, which is an analytic QCD model with exceptionally fast convergence properties, the more simple approach (2/1-loop) gives the results close to (within a few per cent) the approaches using the higher-loop versions for the underlying pQCD. Therefore, in FAPT model, we can use various levels (2/1-, 3/2- and 4/3-loop), while for the other two versions of analytic QCD (2 δ anQCD and MPt) the preferred versions are 4/3-loop.

In addition, in FAPT, the program allows to choose either the usual version (i.e., at a fixed chosen N_f), or a “global” version [19] for which the underlying pQCD coupling $a(Q^2; N_f)$ [and its discontinuity function $\rho_1^{(N_f, \text{pt})}(\sigma) \equiv \text{Im}a(-\sigma - i\epsilon; N_f)$] is replaced by a new, “global”, pQCD coupling

$$a^{(\text{glob.})}(Q^2) = a(Q^2; N_f = 3; \overline{\Lambda}_3)\Theta(|Q^2| \leq \mu^{(4)2}) + a(Q^2; N_f = 4; \overline{\Lambda}_4)\Theta(\mu^{(4)2} < |Q^2| \leq \mu^{(5)2}) \\ + a(Q^2; N_f = 5; \overline{\Lambda}_5)\Theta(\mu^{(5)2} < |Q^2| \leq \mu^{(6)2}) + a(Q^2; N_f = 6; \overline{\Lambda}_6)\Theta(\mu^{(6)2} < |Q^2|) \quad (18)$$

where $\mu^{(3)} = \kappa m_3 = \kappa \overline{m}_c(\overline{m}_c)$, etc., and the scales $\overline{\Lambda}_{N_f}$ and the RGE-running of $a(Q^2; N_f)$ are determined by $N/(N - 1)$ -loop approach in $\overline{\text{MS}}$ (in the following referred to simply as N -loop approach; $N = 1, 2, 3, 4$). However, in such a global FAPT the values of the scales $\overline{\Lambda}_{N_f}$ differ somewhat from those of the actually valid pQCD [in the latter, the world average value $a(M_Z^2; 5) = 0.1184/\pi$ in $\overline{\text{MS}}$ scheme fixes the scale $\overline{\Lambda}_5$, see Table 1]. The preferred values in the global FAPT are $\overline{\Lambda}_5 \approx 0.260$ GeV [19, 22, 23, 43], corresponding to $\overline{\Lambda}_3 \approx 0.435$ GeV [and $\alpha_s(M_Z^2; 5; \overline{\text{MS}}) \approx 0.1218$] in 2/1-loop approach with $\kappa = 2$, and to $\overline{\Lambda}_3 \approx 0.400$ GeV in 4/3-loop approach with $\kappa = 2$.

3. Analytic QCD models

3.1. General formalism

In analytic QCD models, the dispersion relation between the discontinuity function $\rho_1(\sigma) \equiv \text{Im}\mathcal{A}_1(-\sigma - i\epsilon)$ and the coupling itself $\mathcal{A}_1(Q^2)$ plays usually a fundamental role, where the discontinuity function $\rho_1(\sigma)$ is proportional to the discontinuity of \mathcal{A}_1 across the cut at $Q^2 = -\sigma (< 0)$. In pQCD such dispersion relation also exists. Namely, when the function $a(Q'^2)/(Q'^2 - Q^2)$ is integrated in the Q'^2 complex plane along an appropriate closed contour which avoids all the cuts and encloses the pole $Q'^2 = Q^2$ (cf. Fig. 2(a)), and the Cauchy theorem is applied, the following dispersion relation is obtained:

$$a(Q^2) = \frac{1}{\pi} \int_{\sigma=-\Lambda_{\text{Lan.}}^2}^{\infty} \frac{d\sigma \rho_1^{(\text{pt})}(\sigma)}{(\sigma + Q^2)}, \quad (\eta \rightarrow +0). \quad (19)$$

Here, $\rho_1^{(\text{pt})}(\sigma) \equiv \text{Im}a(-\sigma - i\epsilon)$ is the discontinuity function of the pQCD coupling a along the entire cut axis, and $Q'^2 = \Lambda_{\text{Lan.}}^2 (> 0)$ is the branching point of the Landau cut of the

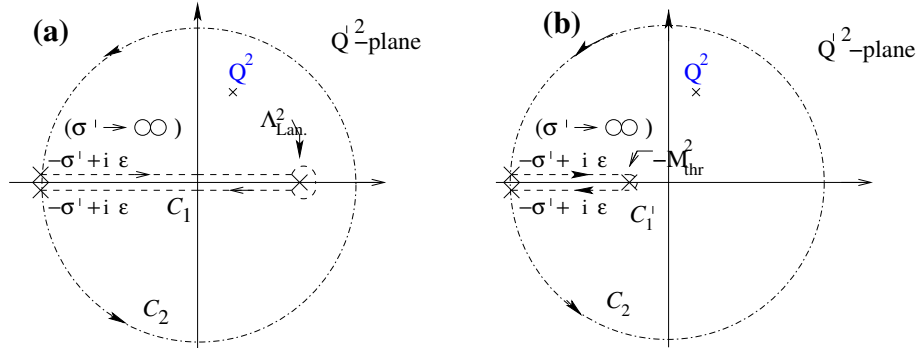


Figure 2: (a) The integration contour for the integrand $a(Q'^2)/(Q'^2 - Q^2)$ leading to the dispersion relation (19) for $a(Q^2)$; (b) the integration contour for the integrand $\mathcal{A}(Q'^2)/(Q'^2 - Q^2)$ of a holomorphic coupling $\mathcal{A}(Q^2)$ leading to the dispersion relation (20). The radius of the circular section tends to infinity.

pQCD coupling $a(Q^2)$.

In general analytic QCD models the dispersion relation has the form

$$\mathcal{A}_1(Q^2) = \frac{1}{\pi} \int_{\sigma=M_{\text{thr}}^2}^{\infty} \frac{d\sigma \rho_1(\sigma)}{(\sigma + Q^2)}, \quad \text{where : } \rho_1(\sigma) \equiv \text{Im}\mathcal{A}_1(-\sigma - i\epsilon). \quad (20)$$

The discontinuity function $\rho_1(\sigma)$ is defined for $\sigma \geq 0$; usually, the discontinuity cut is nonzero below a threshold value $-\sigma \leq -M_{\text{thr}}^2$ where $M_{\text{thr}} \sim M_\pi$. Therefore Q^2 can have any value in the complex plane except on the cut $(-\infty, -M_{\text{thr}}^2]$ (cf. Fig. 2(b)).

We regard either the discontinuity function $\rho_1(\sigma)$, or the coupling function $\mathcal{A}_1(Q^2)$, as the quantity which defines the anQCD model. Below we describe how one constructs from them other quantities, such as analytic analogs $\mathcal{A}_\nu(Q^2)$ of powers $a(Q^2)^\nu$ (where ν is a real number) once the function $\rho_1(\sigma)$ or $\mathcal{A}_1(Q^2)$ is known.

In order to find the correct analogs \mathcal{A}_n of the powers a^n , the logarithmic derivatives are needed

$$\tilde{\mathcal{A}}_{n+1}(Q^2) \equiv \frac{(-1)^n}{\beta_0^n n!} \left(\frac{\partial}{\partial \ln Q^2} \right)^n \mathcal{A}_1(Q^2), \quad (n = 0, 1, 2, \dots). \quad (21)$$

We note that for $n = 0$ we have $\tilde{\mathcal{A}}_1 \equiv \mathcal{A}_1$. We can write the logarithmic derivatives in the following form [46]:

$$\tilde{\mathcal{A}}_{n+1}(Q^2) = \frac{1}{\pi} \frac{(-1)^n}{\beta_0^n \Gamma(n+1)} \int_0^\infty \frac{d\sigma}{\sigma} \rho_1(\sigma) \text{Li}_{-n}(-\sigma/Q^2). \quad (22)$$

This relation is valid for $n = 0, 1, 2, \dots$. Analytic continuation in $n \mapsto \nu$ ($\nu \in \Re$) gives us⁵ the logarithmic noninteger derivatives [46]

$$\tilde{\mathcal{A}}_{\nu+1}(Q^2) = \frac{1}{\pi} \frac{(-1)^\nu}{\beta_0^\nu \Gamma(\nu+1)} \int_0^\infty \frac{d\sigma}{\sigma} \rho_1(\sigma) \text{Li}_{-\nu} \left(-\frac{\sigma}{Q^2} \right) \quad (-1 < \nu). \quad (23)$$

We note that the integral converges for $\nu > -1$. Namely, at high σ ($|z| \gg 1$ where $z \equiv \sigma/Q^2$) we have in the integrand of equation (23): $\rho_1(\sigma) \approx \rho_1^{(\text{pt})}(\sigma) \sim \ln^{-2} \sigma \sim \ln^{-2} z$ and $\text{Li}_{-\nu}(-z) \sim \ln^{-\nu} z$ (for noninteger ν). Therefore, the integral converges at $\sigma \rightarrow \infty$ if $\nu > -1$. The integral obviously converges at low σ , too.⁶

We can recast the result (23) into an alternative form involving the spacelike coupling \mathcal{A}_1 instead of the discontinuity function $\rho_1(\sigma)$. This gives us (for $\nu = n + \delta$, with $0 < \delta < 1$ and $n = -1, 0, 1, 2, \dots$) [46]

$$\begin{aligned} \tilde{\mathcal{A}}_{\nu+1}(Q^2) &\equiv \tilde{\mathcal{A}}_{n+1+\delta}(Q^2) \\ &= \frac{1}{\beta_0^\nu \Gamma(1+\nu) \Gamma(1-\delta)} \left(-\frac{d}{d \ln Q^2} \right)^{n+1} \int_0^1 \frac{d\xi}{\xi} \mathcal{A}_1(Q^2/\xi) \ln^{-\delta} \left(\frac{1}{\xi} \right) \end{aligned} \quad (24a)$$

$$= \frac{1}{\beta_0^\nu} \frac{\Gamma(1+\delta)}{\Gamma(n+1+\delta)} \frac{\sin(\pi\delta)}{(\pi\delta)} \left(-\frac{d}{d \ln Q^2} \right)^{n+1} \int_0^\infty \frac{dt}{t^\delta} \mathcal{A}_1(Q^2 e^t), \quad (24b)$$

where the last form (24b) was obtained from the previous one by the substitution $t = \ln(1/\xi)$ and using the identity $\Gamma(1+\delta)\Gamma(1-\delta) = \pi\delta/\sin(\pi\delta)$.

The analytic analogs $\mathcal{A}_\nu(Q^2) \equiv (a^\nu(Q^2))_{\text{an}}$ of powers $a(Q^2)^\nu$ can be constructed as linear combinations of $\tilde{\mathcal{A}}_{\nu+m}$'s:

$$\mathcal{A}_\nu = \tilde{\mathcal{A}}_\nu + \sum_{m \geq 1} \tilde{k}_m(\nu) \tilde{\mathcal{A}}_{\nu+m}, \quad (25)$$

⁵ In **Mathematica** [60], the $\text{Li}_{-\nu}(z)$ function is implemented as $\text{PolyLog}[-\nu, z]$. However, in **Mathematica** 9.0.1, at large $|z| > 10^7$, $\text{PolyLog}[-\nu, z]$ is unstable. For such z we should use the identities relating $\text{Li}_{-\nu}(z)$ with $\text{Li}_{-\nu}(1/z)$, which can be found, for example, in [61]. Our supplementary module `Li_nu.m` gives such stable functions $\text{Li}_{-\nu}(z) = \text{polylog}[-\nu, z]$. In **Mathematica** 10.0.1 this problem is solved.

⁶A related, but somewhat lengthier, formula for $\tilde{\mathcal{A}}_{\nu+1}(Q^2)$ in terms of $\rho_1(\sigma)$ which is valid in an extended interval ($-2 < \nu$), was also obtained in Ref. [46] [cf. Eq.(22) there]. Our **Mathematica** package uses that lengthy formula.

where the coefficients $\tilde{k}_m(\nu)$ were obtained in [46] for general ν .

The approach (23) with (25) [\Leftrightarrow (24) with (25)] for the case of integer ν was constructed in Refs. [27, 28], and for general real ν in Ref. [46].

Specifically, let us consider a general spacelike scale- and scheme-invariant physical quantity $\mathcal{D}(Q^2)$ which has the available truncated perturbation (power) series of the form

$$\mathcal{D}^{[N]}(Q^2; \kappa)_{\text{pt}} = a(\kappa Q^2)^{\nu_0} + d_1(\kappa)a(\kappa Q^2)^{\nu_0+1} + \dots + d_{N-1}(\kappa)a(\kappa Q^2)^{\nu_0+N-1}, \quad (26)$$

where $0 < \kappa \sim 1$ is the renormalization scale parameter. The evaluation of this quantity in a general analytic QCD model is then performed by the substitution $a^{\nu_0+n} \mapsto \mathcal{A}_{\nu_0+n}$

$$\mathcal{D}^{[N]}(Q^2; \kappa)_{\text{an}} = \mathcal{A}_{\nu_0}(\kappa Q^2) + d_1(\kappa)\mathcal{A}_{\nu_0+1}(\kappa Q^2) + \dots + d_{N-1}(\kappa)\mathcal{A}_{\nu_0+N-1}(\kappa Q^2), \quad (27)$$

with the quantities \mathcal{A}_{ν_0+n} constructed according to Eq. (25) where the truncations are made, in general, at the highest available order of the series (26), i.e., at $\sim a^{\nu_0+N-1} \sim \tilde{\mathcal{A}}_{\nu_0+N-1}$

$$\mathcal{A}_{\nu_0+n} = \tilde{\mathcal{A}}_{\nu_0+n} + \sum_{m=1}^{N-1-n} \tilde{k}_m(\nu_0+n)\tilde{\mathcal{A}}_{\nu_0+n+m}. \quad (28)$$

We refer for more details to Refs. [46, 62]. It is important to note that $\mathcal{A}_{\nu_0+n} \neq (\mathcal{A}_1)^{\nu_0+n}$, i.e., the series (27) is a nonpower series in any analytic QCD which is not perturbative. If, instead, we used in such analytic QCD the powers $(\mathcal{A}_1)^{\nu_0+n}$, the resulting truncated power series would show increased renormalization scale dependence and (for low $|Q^2|$) strongly divergent behavior when N increases, a consequence of incorrect treatment of the nonperturbative contributions contained in the difference $\mathcal{A}_1(\mu^2) - a(\mu^2)$, as emphasized in Refs. [62].

Further, the result (27)-(28) can be reexpressed in terms of $\tilde{\mathcal{A}}_{\nu_0+n}$'s

$$\mathcal{D}^{[N]}(Q^2; \kappa)_{\text{an}} = \tilde{\mathcal{A}}_{\nu_0}(\kappa Q^2) + \tilde{d}_1(\kappa)\tilde{\mathcal{A}}_{\nu_0+1}(\kappa Q^2) + \dots + \tilde{d}_{N-1}(\kappa)\tilde{\mathcal{A}}_{\nu_0+N-1}(\kappa Q^2), \quad (29)$$

where

$$\tilde{d}_M(\kappa) = d_M(\kappa) + \sum_{q=1}^M \tilde{k}_q(\nu_0+M-q)d_{M-q}(\kappa), \quad (M = 1, 2, \dots, N-1), \quad (30)$$

and the convention $d_0(\kappa) = 1$ is taken. Comparing the expressions (27) and (29), it becomes clear that in anQCD the basic quantities in perturbation expansion are the (generalized) logarithmic derivatives $\tilde{\mathcal{A}}_\nu$, and not the (nonpower) analogs \mathcal{A}_ν of pQCD powers a^ν . These aspects have been presented and emphasized in more detail in Refs. [62].

When we evaluate a timelike physical quantity $\mathcal{F}(\sigma)$, such a quantity can be expressed as a contour integral of the corresponding spacelike quantity $\mathcal{D}(Q^2)$ in the complex Q^2 plane. Therefore, $\mathcal{F}(\sigma)$ can be expressed as a series of contour integrals of the couplings $\mathcal{A}_\nu(Q^2)$ or $\tilde{\mathcal{A}}_\nu(Q^2)$.

3.2. Fractional Analytic Perturbation Theory (FAPT)

The APT procedure [16] is the elimination of the contributions of the Landau cut $0 < (-\sigma) \leq \Lambda_{\text{Lan.}}^2$. This gives the APT analytic analog $\mathcal{A}_1^{(\text{APT})}(Q^2; N_f)$ of $a(Q^2; N_f)$

$$\mathcal{A}_1^{(\text{APT})}(Q^2; N_f) = \frac{1}{\pi} \int_{\sigma=0}^{\infty} \frac{d\sigma \rho_1^{(\text{pt})}(\sigma; N_f)}{(\sigma + Q^2)}. \quad (31)$$

This procedure can be extended to the construction of the APT-analogs $\mathcal{A}_n^{(\text{APT})}(Q^2)$ of n -integer powers $a(Q^2)^n$ [17, 19] and their combinations (see also [63]). The APT analogs of general powers a^ν (ν a real exponent) are known as Fractional APT (FAPT) [20–23]; following the same procedure, they are

$$\mathcal{A}_\nu^{(\text{FAPT})}(Q^2; N_f) = \frac{1}{\pi} \int_{\sigma=0}^{\infty} \frac{d\sigma \rho_\nu^{(\text{pt})}(\sigma; N_f)}{(\sigma + Q^2)}, \quad (32)$$

where

$$\rho_\nu^{(\text{pt})}(\sigma; N_f) = \text{Im } a(Q'^2 = -\sigma - i\epsilon; N_f)^\nu. \quad (33)$$

It turns out that in FAPT, where the approach (32) can be applied,⁷ it is equivalent with the approach of Eqs. (23) and (25) [or, equivalently, Eqs. (24) and (25)] that can be applied in general anQCD models, if in the sums on the right-hand side of Eq. (25) we do not make truncations of the type of Eq. (28), but rather include as many terms as possible. We refer to Refs. [27, 28, 46] for more details on these points.

In the global version of FAPT, the coupling $\mathcal{A}_\nu^{(\text{FAPT})\text{glob.}}(Q^2)$ is obtained by applying the dispersion relation to the discontinuity function of the power ν of the global coupling (18), for $\sigma \geq 0$

$$\begin{aligned} \rho_\nu^{(\text{pt})\text{glob.}}(\sigma) &= \text{Im } a^{(\text{glob.})}(Q^2 = -\sigma - i\epsilon)^\nu \\ &\equiv \rho_\nu^{(\text{pt})}(\sigma; \bar{\Lambda}_3) \Theta(|Q^2| \leq \mu^{(4)2}) + \rho_\nu^{(\text{pt})}(\sigma; \bar{\Lambda}_4) \Theta(\mu^{(4)2} \leq |Q^2| \leq \mu^{(5)2}) + \\ &\quad \rho_\nu^{(\text{pt})}(\sigma; \bar{\Lambda}_5) \Theta(\mu^{(5)2} \leq |Q^2| \leq \mu^{(6)2}) + \rho_\nu^{(\text{pt})}(\sigma; \bar{\Lambda}_6) \Theta(\mu^{(6)2} \leq |Q^2|). \end{aligned} \quad (34)$$

If the underlying pQCD running coupling $a(Q^2)$ runs according to the one-loop perturbative RGE, the corresponding explicit expressions for $\mathcal{A}_\nu^{(\text{FAPT})}$ exist and were obtained and used in Ref. [20]

$$\mathcal{A}_\nu(Q^2)^{(\text{FAPT}, 1-\ell)} = \frac{1}{\beta_0^\nu} \left(\frac{1}{\ln^\nu(z)} - \frac{\text{Li}_{-\nu+1}(1/z)}{\Gamma(\nu)} \right). \quad (35)$$

⁷ We note that in anQCD models other than FAPT as defined by Eq. (31), the approach of the type (32) to the calculation of \mathcal{A}_ν 's is not applicable. This is so because in such anQCD models $\rho_1(\sigma) \equiv \text{Im} \mathcal{A}_1(-\sigma - i\epsilon) [\neq \text{Im} a(-\sigma - i\epsilon)]$ and, for $\nu \neq 1$ we have: $\rho_\nu(\sigma) \equiv \text{Im} \mathcal{A}_\nu(-\sigma - i\epsilon)$. Therefore, $\rho_\nu(\sigma) \neq \text{Im} a(-\sigma - i\epsilon)^\nu$ and $\rho_\nu(\sigma) \neq \text{Im} \mathcal{A}_1(-\sigma - i\epsilon)^\nu$. The former inequality holds because the model is not FAPT; the latter inequality holds because $\mathcal{A}_\nu \neq \mathcal{A}_1^\nu$ (for $\nu \neq 1$) in general anQCD models which are simultaneously not pQCD. For models which are anQCD and simultaneously pQCD (i.e., anpQCD), we refer to Refs. [64].

Here, $z \equiv Q^2/\Lambda^2$ and $\text{Li}_{-\nu+1}(x)$ is the polylogarithm function of order $-\nu + 1$. Explicit extensions to approximate higher loops were performed by expanding the one-loop result in a series of derivatives with respect to the index ν [20, 22, 23]⁸ We refer for reviews of FAPT to Refs. [43–45].

When in FAPT the underlying pQCD coupling $a(Q^2)$ is given by Eqs. (4) and (11), the resulting theory is called 1-loop and 2-loop FAPT, respectively. When $a(Q^2)$ is given by Eq. (14) with $c_2 = \bar{c}_2(N_f)$ of $\overline{\text{MS}}$ scheme, the resulting theory is called, somewhat loosely, 3-loop FAPT. When $a(Q^2)$ is given by the expansion (6), with $c_2 = \bar{c}_2(N_f)$ and $c_3 = \bar{c}_3(N_f)$ ($c_j = 0$ for $j \geq 4$; and the truncation index $\mathcal{N} = 8$ is used), the resulting FAPT is called 4-loop.

Due to easiness of numerical implementation, in this model we incorporate the FAPT-analytization of logarithmic powers, too

$$\mathcal{A}_{\nu,k}^{(\text{FAPT})}(Q^2) = \frac{1}{\pi} \int_{\sigma=0}^{\infty} \frac{d\sigma \text{Im} [a(-\sigma - i\epsilon)^\nu \ln^k a(-\sigma - i\epsilon)]}{(\sigma + Q^2)}, \quad (36)$$

where ν is a general (noninteger) index and $k = 0, 1, 2, \dots$

The couplings of FAPT_{N_f} and of global FAPT are calculated also in the `Mathematica` program of Ref. [48]. The values of couplings $\mathcal{A}_\nu(Q^2)$ of FAPT_{N_f} models in our program, when $\kappa = 2$ is changed there to $\kappa = 1$, practically coincide with the corresponding values of [48]. In global FAPT,⁹ there are small differences between our values and theirs, which tend to increase somewhat when ν increases: for $\nu < 1$ the differences are 1% or less, for $1 < \nu < 2$ are 1-2%, for $2 < \nu < 3$ are 2-3%, for $3 < \nu < 4$ are 4-8%. We note, however, that with increasing ν the couplings in FAPT decrease very fast. We believe that one of the principal reasons for the small mentioned differences lies in the fact that in our program the quark thresholds (with $\kappa = 1$) are implemented at the masses \overline{m}_q while in the program of Ref. [48] at the quark pole masses.

Furthermore, the couplings of (F)APT $_{N_f}$ are calculated also by the programs of Ref. [47], in Maple and in Fortran, and their values practically coincide with ours.

3.3. Two-delta analytic model ($2\delta\text{anQCD}$)

3.3.1. $2\delta\text{anQCD}$ in low momentum regime ($N_f = 3$)

In this anQCD model [31], the discontinuity function $\rho_1(\sigma) \equiv \text{Im} \mathcal{A}_1(Q^2 = -\sigma - i\epsilon)$ (for $\sigma > 0$) agrees with the perturbative counterpart $\rho_1^{(\text{pt})}(\sigma) \equiv \text{Im} a(Q^2 = -\sigma - i\epsilon)$ at sufficiently high scales $\sigma \geq M_0^2$ ($M_0^2 \sim 1 \text{ GeV}^2$); while in the low-scale regime $0 < \sigma < M_0^2$ its otherwise unknown behavior is parametrized as a linear combination of (two) delta functions (a parametrization motivated by the Padé approximation approach for

⁸ For practical purposes, we use in the integral (32) the N -loop level $\rho_\nu^{(\text{pt})}(\sigma)$ (where: $N \leq 4$).

⁹ We note that our \mathcal{A}_ν corresponds to their \mathcal{A}_ν/π^ν ; and what we call (approximate) 3-loop (“3l”) they call more rigorously 3-loop-Padé (“3P”).

the running coupling [65])

$$\rho_1^{(2\delta)}(\sigma; c_2) = \pi \sum_{j=1}^2 f_j^2 \Lambda^2 \delta(\sigma - M_j^2) + \Theta(\sigma - M_0^2) \times \rho_1^{(\text{pt})}(\sigma; c_2) \quad (37a)$$

$$= \pi \sum_{j=1}^2 f_j^2 \delta(s - s_j) + \Theta(s - s_0) \times r_1^{(\text{pt})}(s; c_2), \quad (37b)$$

where we define the dimensionless quantities: $s = \sigma/\Lambda^2$, $s_j = M_j^2/\Lambda^2$ ($j = 0, 1, 2$), and $r_1^{(\text{pt})}(s; c_2) = \rho_1^{(\text{pt})}(\sigma; c_2) = \text{Im} a(Q^2 = -\sigma - i\epsilon; c_2)$. Here, Λ^2 ($\lesssim 10^{-1} \text{ GeV}^2$) is the Lambert scale appearing in the expression (14) for a [cf. also Eq. (12)]. The underlying pQCD coupling is taken in the form (14) where the scheme parameter c_2 ($\equiv \beta_2/\beta_0$) is nonzero in general [cf. Eqs. (13)].

The aforementioned branching point of nonanalyticity $z = -1/e$ corresponds, according to Eq. (12), to the scale $Q^2 = \Lambda^2 s_L$ with $s_L = c_1^{-c_1/\beta_0}$ ($= 0.6347$ when $N_f = 3$). The interval of Landau singularities of $a(Q^2)$ of Eq. (14) is: $0 < Q^2 < \Lambda^2 s_L$. In our case we will choose c_2 to be negative. In such a case there is an additional pole-type Landau singularity, at a somewhat higher scale $Q^2 = \Lambda^2 u_L$ – there the denominator in Eq. (14) becomes zero, cf. Fig. 1(b). Our preferred choice of the scheme in the model will be $c_2 = -4.9$; in this case we have $u_L = 1.0311$ ($> s_L$). For this “canonical” case, the underlying pQCD discontinuity function $\rho_1^{(\text{pt})}(\sigma)$ is presented in Fig. 3(a) as a function of σ , and the corresponding $2\delta\text{anQCD}$ discontinuity function $\rho_1^{(2\delta)}(\sigma)$ in Fig. 3(b). The Lambert Λ scale, appearing in Eq. (12), was taken with the value of $\Lambda = 0.255 \text{ GeV}$ because this then corresponds to the world average value $a(M_Z^2; \overline{\text{MS}}) = 0.1184/\pi$, as will be seen later.

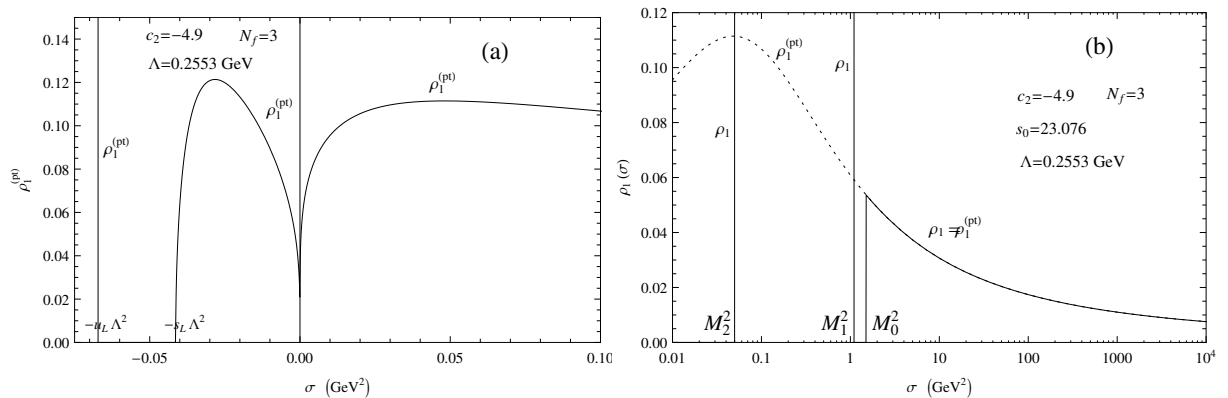


Figure 3: (a) The discontinuity function $\rho_1^{(\text{pt})}(\sigma) \equiv \text{Im} a(-\sigma - i\epsilon)$ of the perturbative coupling a of Eq. (14), for $c_2 = -4.9$ and $N_f = 3$; (b) the corresponding $2\delta\text{anQCD}$ discontinuity function $\rho_1^{(2\delta)}(\sigma)$, Eq. (37a). The MPT discontinuity function is $\rho_1^{(\text{MPT})}(\sigma) = \rho_1^{(\text{pt})}(\sigma - m_{\text{gl}}^2)$, cf. Eq. (45); when $m_{\text{gl}}^2 = 0.7 \text{ GeV}^2$, this is just the curve of Fig. (a) shifted by 0.7 GeV^2 toward the right.

In Fig. 3(a) we see that $a(Q^2; N_f)$, for $c_2 = -4.9$, has a Landau pole at σ ($\equiv -Q^2$) $= -u_L \Lambda^2$ ($\approx -0.067 \text{ GeV}^2$) and the Landau branching point at $\sigma = -s_L \Lambda^2$

($\approx -0.041 \text{ GeV}^2$). Therefore, the dispersive relation (19) for the underlying perturbative coupling $a(Q^2; N_f = 3)$ obtains a slightly generalized form [in comparison with Eq. (19)]

$$a(Q^2) = \frac{1}{\pi} \int_{s=-s_L-\eta}^{\infty} ds \frac{r_1^{(\text{pt})}(s; c_2)}{(s + Q^2/\Lambda^2)} + \frac{\text{Res}_{(z=u_L)} a(z\Lambda^2; c_2)}{(-u_L + Q^2/\Lambda^2)}, \quad (38)$$

which is obtained by application of the Cauchy theorem to the function $a(Q'^2)/(Q'^2 - Q^2)$ along the contour depicted in Fig. 4 [in contrast to the simple contour Fig. 2(a) leading to Eq. (19)].

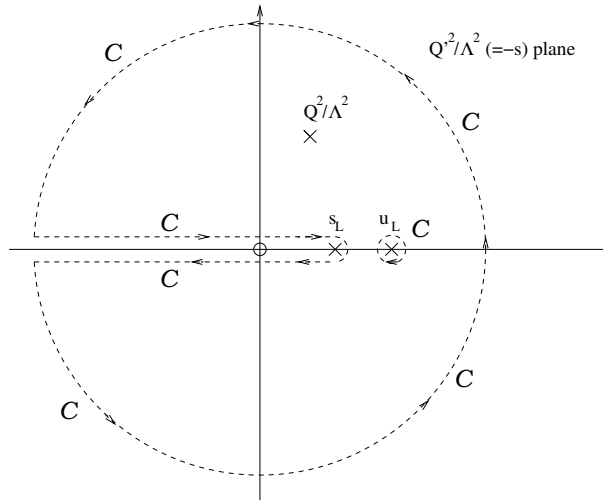


Figure 4: The integration contour for the integrand $a(Q'^2)/(Q'^2 - Q^2)$ leading to the dispersion relation (38) for $a(Q^2)$ of Eq. (14) with $c_2 < 0$. The radius of the large circular section tends to infinity.

The perturbative discontinuity function $r_1^{(\text{pt})}(s; c_2) = \text{Im } a(Q^2 = -s\Lambda^2 - i\epsilon; c_2)$, which is nonzero for $-s_L < s < +\infty$ and at $s = -u_L$, has the specific form

$$r_1^{(\text{pt})}(s; c_2) = \begin{cases} \text{Im} \left[\frac{(-1)}{c_1} \frac{1}{[1 - (c_2/c_1^2) + W_{+1} \left(\frac{-1}{c_1 e} |s|^{-\beta_0/c_1 - i\epsilon} \right)]} \right] & (s < 0), \\ \text{Im} \left[\frac{(-1)}{c_1} \frac{1}{[1 - (c_2/c_1^2) + W_{+1} \left(\frac{-1}{c_1 e} |s|^{-\beta_0/c_1} \exp(i\beta_0\pi/c_1) \right)]} \right] & (s > 0). \end{cases} \quad (39)$$

The analytic (spacelike) coupling $\mathcal{A}_1^{(2\delta)}(Q^2; c_2)$ of the two-delta anQCD model is constructed on the basis of the discontinuity function (37) [cf. Eq. (39) for $s > 0$] using the dispersion relation. This gives

$$\mathcal{A}_1^{(2\delta)}(Q^2; c_2) = \sum_{j=1}^2 \frac{f_j^2}{(s_j + u)} + \frac{1}{\pi} \int_{s_0}^{\infty} ds \frac{r_1^{(\text{pt})}(s; c_2)}{(s + u)}, \quad (40)$$

where $u = Q^2/\Lambda^2$.

In the Two-delta $N_f = 3$ anQCD model with a chosen value of c_2 [$2\delta\text{anQCD}_{N_f=3}(c_2)$], and with $c_1 = c_1(N_f = 3) = (\beta_1/\beta_0)_{N_f=3}$, the first three quark flavors are approximated

as massless. Most importantly, the model is constructed so that at high $|Q^2|$ it basically coincides with the underlying pQCD $_{N_f=3}(c_2)$, and that it simultaneously reproduces the experimental value of the (canonical) decay ratio r_τ of the strangeless and massless ($V + A$)-channel semihadronic decays of the τ lepton: $r_\tau = 0.203$. This is achieved in three steps.

1. The first step is to obtain the value of the Lambert scale Λ appearing in the underlying pQCD $_{N_f=3}(c_2)$ coupling $a(Q^2)$ of Eqs. (14) and (12). This is done in the following way: the world average value $\bar{a}(M_Z^2) = 0.1184/\pi$ is evolved by 4-loop $\overline{\text{MS}}$ RGE from $Q^2 = M_Z^2$ down to $Q^2 = (2\bar{m}_c)^2$, obtaining $\bar{a}_{\text{in}} \equiv \bar{a}((2\bar{m}_c)^2; N_f = 3) = 0.26535/\pi$. 3-loop threshold matching (16) is used, at $Q^2 = (2\bar{m}_b)^2$ and $(2\bar{m}_c)^2$ ($\bar{m}_b = 4.2$ GeV and $\bar{m}_c = 1.27$ GeV). From this value \bar{a}_{in} , in $\overline{\text{MS}}$ scheme, the corresponding value $a_{\text{in}} \equiv a((2m_c)^2; c_2, c_2^2/c_1, \dots; N_f = 3)$ in the renormalization scheme of the $2\delta\text{anQCD}_{N_f=3}(c_2)$ model is obtained, i.e., in the scheme determined by the beta function $\beta(a)$ of Eq. (13). This is performed by solving for a_{in} the integrated form of RGE (i.e., implicit solution) in its subtracted form, cf. Appendix A of Ref. [51] (cf. also Appendix A of Ref. [66])

$$\frac{1}{a_{\text{in}}} + c_1 \ln \left(\frac{c_1 a_{\text{in}}}{1 + c_1 a_{\text{in}}} \right) + \int_0^{a_{\text{in}}} dx \left[\frac{\beta(x) + \beta_0 x^2 (1 + c_1 x)}{x^2 (1 + c_1 x) \beta(x)} \right] = \frac{1}{\bar{a}_{\text{in}}} + c_1 \ln \left(\frac{c_1 \bar{a}_{\text{in}}}{1 + c_1 \bar{a}_{\text{in}}} \right) + \int_0^{\bar{a}_{\text{in}}} dx \left[\frac{\bar{\beta}(x) + \beta_0 x^2 (1 + c_1 x)}{x^2 (1 + c_1 x) \bar{\beta}(x)} \right]. \quad (41)$$

For $c_2 = -4.9$ this gives $a_{\text{in}} = 0.24860/\pi$. Equating this value with the expression (14) (with $c_2 = -4.9$ and $N_f = 3$) gives the Lambert scale $\Lambda \equiv \Lambda_3$ of the model: $\Lambda = 0.2553$ GeV. For other values of c_2 , other values of Λ are obtained.

2. The second step is to make the model $2\delta\text{anQCD}_{N_f=3}(c_2)$ practically coincide with the underlying pQCD $_{N_f=3}(c_2)$ at high $|Q^2| > \Lambda^2$. In general, $\mathcal{A}_1(Q^2; c_2)$ differs from $a(Q^2; c_2)$ at $Q^2 > \Lambda^2$ by $\sim (\Lambda^2/Q^2)^1$, as is the case, e.g., with FAPT and MPT. In $2\delta\text{anQCD}$ we impose the condition

$$\mathcal{A}_1(Q^2; c_2) - a(Q^2; c_2) \sim (\Lambda^2/Q^2)^{n_{\text{max}}} \quad \text{with } n_{\text{max}} = 5. \quad (42)$$

The condition (42) represents in practice four conditions, which fix four dimensionless parameters s_j, f_j^2 ($j = 1, 2$) in terms of the fifth dimensionless parameter s_0 .

3. The third step is to ensure that the model $2\delta\text{anQCD}_{N_f=3}(c_2)$ reproduces the correct central value of the ($V + A$)-channel semihadronic τ decay ratio¹⁰ $r_\tau(\Delta S = 0, m_q = 0)_{\text{exp}} = 0.203 \pm 0.004$.

¹⁰This quantity is normalized canonically, i.e., its perturbation expansion is $(r_\tau)_{\text{pt}} = a + \mathcal{O}(a^2)$. For details on r_τ and its evaluation in analytic QCD approaches, we refer to Ref. [31] and Appendices B-E of Ref. [64].

Table 2: Values of the parameters of the considered $2\delta\text{anQCD}$ model, for $N_f = 3$ and $-5.6 \leq c_2 \leq -2.0$. We consider $c_2 = -4.9$ ($M_0 \approx 1.23$ GeV) as the preferred representative case. The value $\pi \times a_{\text{in}} = \alpha_s((2m_c)^2; c_2, \dots; N_f = 3)$ and the Lambert scale value Λ in the corresponding cases are for the QCD coupling parameter value $\alpha_s^{(\overline{\text{MS}})}(M_Z^2) = 0.1184$.

c_2	$\pi \times a_{\text{in}}$	Λ [GeV]	s_0	s_1	f_1^2	s_2	f_2^2	M_0	$\mathcal{A}_1(0)$
-5.60	0.2477	0.2339	24.416	17.787	0.3013	0.6906	0.6150	1.156	0.9999
-5.40	0.2480	0.2398	24.054	17.533	0.2936	0.7179	0.5960	1.176	0.9389
-4.90	0.2486	0.2552	23.076	16.839	0.2746	0.7688	0.5505	1.226	0.8231
-4.00	0.2498	0.2857	21.142	15.454	0.2416	0.8094	0.4753	1.314	0.6916
-3.00	0.2512	0.3237	18.903	13.836	0.2078	0.8003	0.4020	1.407	0.6042
-2.00	0.2526	0.3668	16.708	12.241	0.1775	0.7557	0.3388	1.499	0.5481

The scheme parameter c_2 ($\equiv \beta_2/\beta_0$) can still be varied. Physical considerations guide us to restrict the preferred values of the pQCD-onset scale M_0 and of the coupling $\mathcal{A}_1(Q^2)$ at $Q^2 = 0$: $M_0 \leq 1.5$ GeV and $\mathcal{A}_1(0) < 1$. This gives us the variation of c_2 in the interval $-5.6 < c_2 < -2, 0$. In Table 2 we present the results for the parameters of the model for various values of c_2 in this interval.¹¹ Our preferred choice is $c_2 = -4.9$ where $M_0 \approx 1.23$ GeV and $\mathcal{A}_1(0) \approx 0.82$.

The (generalized) logarithmic derivatives $\tilde{\mathcal{A}}_\nu$ are then constructed by the procedure (23), and the power analogs \mathcal{A}_ν by the linear combinations (28) (where $\nu_0 = \nu$) with the truncation (“loop”) index there being $N = 1, 2, 3, 4, 5$.

3.3.2. $2\delta\text{anQCD}$ for $N_f \geq 4$

The $2\delta\text{anQCD}$ model can be constructed also for $N_f = 4, 5, 6$. In such cases, for a chosen value of c_2 [$= c_2(N_f)$], the value of Λ_{N_f} is determined by pQCD, as in $N_f = 3$ case. Further, the condition (42) again gives us the values of the four parameters s_j and f_j^2 ($j = 1, 2$) in terms of s_0 . However, since in the case of $N_f \geq 4$ the couplings $\mathcal{A}_\nu(Q^2)$ should be applied only for $|Q^2| > (2m_{N_f})^2$ (where: $m_4 = \bar{m}_c$, $m_5 = \bar{m}_b$, $m_6 = \bar{m}_t$), the low-momentum quantity r_τ cannot and should not be evaluated in such framework. Therefore, for $N_f \geq 4$ the value of the s_0 parameter is free. In our program, we kept the value of $s_0(N_f)$ equal to the corresponding value of $s_0(N_f = 3)$. In such cases, the $N_f = 4$ $2\delta\text{anQCD}$ model still remains formally analytic, while for $N_f = 5, 6$ it is formally nonanalytic (since $s_2 < 0$ is such a case). Nevertheless, we prefer to keep such, relatively low, values of s_0 for $N_f \geq 4$, because then the coefficient on the right-hand side of Eq. (42) in front of $(\Lambda^2/Q^2)^5$ is not very large; therefore, the model for $N_f \geq 4$ practically agrees with the underlying pQCD. The relative difference between $2\delta\text{anQCD}$ values $\mathcal{A}_1(Q^2; N_f)$

¹¹ In Ref. [31], the obtained parameters of the model were slightly different. The principal reason for that was that the 3-loop quark threshold conditions in the $\overline{\text{MS}}$ RGE-running downwards in Ref. [31] were implemented by a version of (16) expressing a as a truncated power series of a' . However, the numerical results for the coupling, at a given c_2 , are almost indistinguishable from those of Ref. [31].

and the corresponding pQCD values $a(Q^2; N_f)$, $\text{rd}(Q^2) \equiv |\mathcal{A}_1(Q^2; N_f)/a(Q^2; N_f) - 1|$, as a function of positive Q^2 and for various N_f , is given in Fig. 5. These differences are extremely small, with the exception of low Q^2 : $0 < Q^2 < 1 \text{ GeV}^2$. When $N_f = 4$, the difference $\mathcal{A}_1(Q^2; N_f)/a(Q^2; N_f) - 1$ changes sign from negative to positive at increasing Q^2 around $Q^2 \approx 17 \text{ GeV}^2$; in the case of $N_f = 5$ this occurs around $Q^2 \approx 6 \text{ GeV}^2$. In the case of $N_f = 3$ we have $\mathcal{A}_1(Q^2; 3)/a(Q^2; 3) - 1 < 0$ for all positive Q^2 . These differences

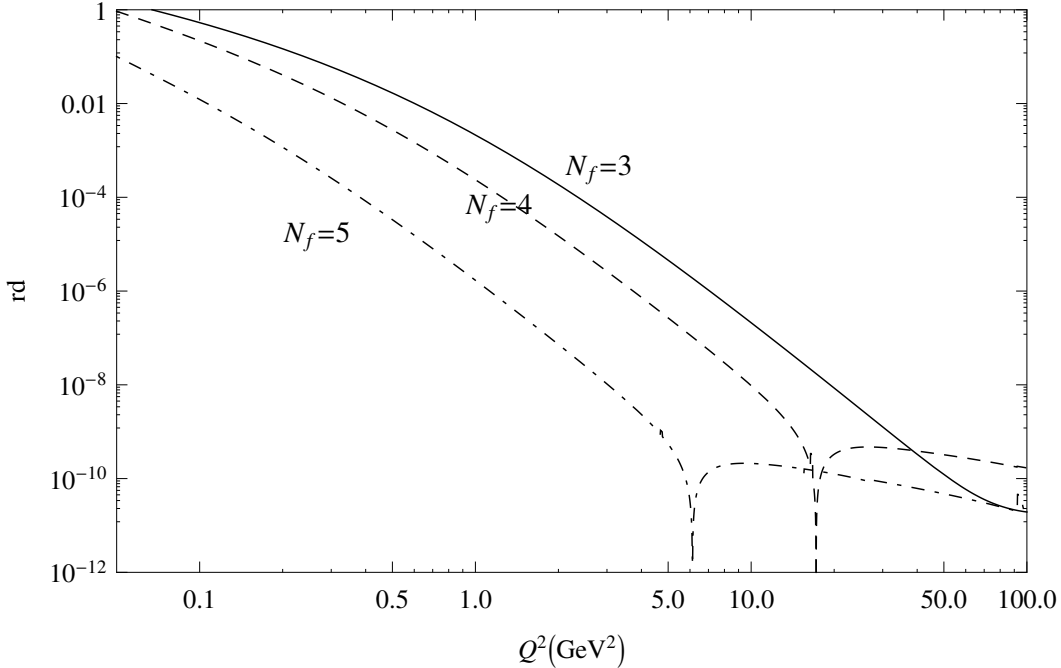


Figure 5: The relative difference between $2\delta\text{anQCD}$ coupling and the underlying pQCD coupling, $\text{rd}(Q^2) \equiv |\mathcal{A}_1(Q^2; N_f)/a(Q^2; N_f) - 1|$, as a function of positive Q^2 , for $N_f = 3, 4, 5$. The parameter c_2 of the model is set equal to $c_2(N_f) = -4.9$.

$\text{rd}(Q^2)$ get smaller when N_f increases. Therefore, the model $2\delta\text{anQCD}$ for $N_f \geq 4$ can be used in practical calculations of the underlying couplings $a(Q^2)$ [$\approx \mathcal{A}_1(Q^2)$] and $\tilde{a}_\nu(Q^2)$ [$\approx \tilde{\mathcal{A}}_\nu(Q^2)$]. We note that for any real $\nu \geq 0$ we have

$$\tilde{\mathcal{A}}_\nu(Q^2; N_f) - \tilde{a}_\nu(Q^2; N_f) \sim \left(\frac{\Lambda_{N_f}^2}{Q^2} \right)^5, \quad (43)$$

which is a consequence of Eq. (42). Namely, for integer $\nu = 2, 3, \dots$ this can be obtained by applying $K_\nu(Q^2 d/dQ^2)^{\nu-1}$ to both sides of Eq. (42), where $K_\nu = (-1)^{\nu-1}/[\beta_0^{\nu-1}(\nu-1)!]$, cf. Eq. (21).¹² And for ν noninteger Eq. (43) follows by analytic continuation of the integer case to ν . We stress that the exact calculation of the pQCD quantities $\tilde{a}_\nu(Q^2; N_f)$ for

¹² We note that in such a case the derivative $(Q^2 d/dQ^2)^{\nu-1}$ applied to $(\Lambda^2/Q^2)^5$ gives $(-5)^{\nu-1}(\Lambda^2/Q^2)^5$.

noninteger ν is quite complicated, due to the Landau singularities of the original pQCD coupling¹³ $a(Q^2; N_f)$. Therefore, in the evaluations of the series of the type

$$\mathcal{D}(Q^2) = a(Q^2)^{\nu_0} + \sum_{m=1}^{\infty} d_m a(Q^2)^{\nu_0+m} \quad (44a)$$

$$= \tilde{a}_{\nu_0}(Q^2) + \sum_{m=1}^{\infty} \tilde{d}_m \tilde{a}_{\nu_0+m}(Q^2) \quad (44b)$$

with ν noninteger, the (truncated) expansion in the generalized logarithmic derivatives (44b) can be evaluated in practice by applying the model $2\delta\text{anQCD}$ (at a given N_f), as explained in Eqs. (26)-(29). The (truncated) series in powers (44a) is, certainly, much easier to evaluate technically than the (truncated) series (44b); nonetheless, the latter series may behave in some cases better than the former, and then $2\delta\text{anQCD}$ can be called upon, with the replacements: $\tilde{a}_{\nu_0+m}(Q^2; N_f) \mapsto \tilde{\mathcal{A}}_{\nu_0+m}^{(2\delta)}(Q^2; N_f)$ and $a(Q^2; N_f)^{\nu_0+m} \mapsto \mathcal{A}_{\nu_0+m}^{(2\delta)}(Q^2; N_f)$. If the quantity $\mathcal{D}(Q^2)$ has low Q^2 corresponding to $N_f = 3$, the evaluation of the (truncated) series (44b) with the model $2\delta\text{anQCD}$ [$\tilde{a}_{\nu_0+m}(Q^2; 3) \mapsto \tilde{\mathcal{A}}_{\nu_0+m}^{(2\delta)}(Q^2; 3)$] is then the natural and the preferred way of evaluation, because the (truncated) series (44) in pQCD are usually numerically badly affected by the vicinity of Landau singularities at such low $|Q^2| < (2\bar{m}_c)^2$.

3.4. Massive Perturbation Theory (MPT)

In order to obtain a holomorphic coupling finite in the infrared regime, the author of Ref. [32] proposed a simple change in the momentum

$$\mathcal{A}_1^{(\text{MPT})}(Q^2; N_f) = a(Q^2 + m_{\text{gl}}^2; N_f) . \quad (45)$$

The mass scale $m_{\text{gl}} \approx 0.5 - 1$ GeV is in this ansatz a constant and is associated with an effective (dynamical) gluon mass which reflects the infrared dynamics of QCD. The same kind of replacement had been suggested, at one- and two-loop level, in Refs. [10, 11] as a result of the use of nonperturbative QCD background. It was used in Refs. [12, 13] in analyses of structure functions (with $m_{\text{gl}} \approx 0.8$ GeV). The relation (45), i.e., the replacement $Q^2 \mapsto Q^2 + m_{\text{gl}}^2$, can be kept even at higher-loop levels, as suggested by the multiplicative renormalizability [67] (and m_{gl}^2 can be expected in general to run with Q^2). Such behavior is suggested also by Gribov-Zwanziger approach [3], by analyses of Dyson-Schwinger equations in QCD [4, 5] and by other functional methods [6, 7].

The coupling (45) is analytic, because $m_{\text{gl}}^2 > \Lambda_{\text{Lan.}}^2$, where $(-q^2 \equiv) Q^2 = -\Lambda_{\text{Lan.}}^2$ is the branching point of the Landau singularity cut of the corresponding pQCD coupling $a(Q^2)$.

¹³ The coupling $\tilde{a}_{\nu+1}(Q^2)$ for integer $\nu = n$ is a simple n 'th logarithmic derivative of $a(Q^2)$, $\tilde{a}_{n+1}(Q^2) \equiv [(-1)^n / (\beta_0^n n!)] (\partial/\partial \ln Q^2)^n a(Q^2)$ [cf. Eq. (21)]. For noninteger ν , $\tilde{a}_{\nu+1}(Q^2)$ could be obtained by a dispersion integral similar to Eq. (23), by including integration over the Landau cuts and poles ($\sigma < 0$). This integration may be complicated, especially if an additional isolated Landau pole is involved as in the case of the coupling (14) with $c_2 < 0$ used here.

Therefore, $\mathcal{A}_1^{(\text{MPT})}(Q^2)$ can be written in the form (20) of dispersion integral, typical in any anQCD. At large $|Q^2|$ the coupling $\mathcal{A}_1^{(\text{MPT})}(Q^2)$ tends to the pQCD coupling $a(Q^2)$, the difference being

$$\mathcal{A}_1^{(\text{MPT})}(Q^2; N_f) - a(Q^2; N_f) \sim \frac{m_{\text{gl}}^2}{Q^2 \ln^2(Q^2/\bar{\Lambda}^2)}. \quad (46)$$

It is important to stress that, as $\mathcal{A}_1^{(\text{MPT})}(Q^2; N_f)$ is a nonperturbative holomorphic coupling, the evaluation of the (truncated) perturbation power series $\mathcal{D}^{[N]}(Q^2)$ of the spacelike scale- and scheme-invariant physical quantities, Eq. (26), should not be performed by replacing $a(\mu^2)^\nu \mapsto \mathcal{A}_1^{(\text{MPT})}(\mu^2)^\nu$, but by the replacement which is obligatory in any anQCD

$$a(\mu^2)^\nu \mapsto \mathcal{A}_\nu(\mu^2), \quad (47)$$

cf. Eq. (27). The nonpower quantities $\mathcal{A}_\nu(\mu^2) = \mathcal{A}_\nu^{(\text{MPT})}(\mu^2)$ are constructed via Eqs. (25) and (24), and in the integrands of Eqs. (24) we use for \mathcal{A}_1 the expression (45). This use of nonpower expressions, based on the (generalized) logarithmic derivatives $\tilde{\mathcal{A}}_{\nu'}(\mu^2)$ presented by Eq. (23) or Eq. (24), has been emphasized in Refs. [27, 28, 32] for the case of integer ν , extended to the case of general (noninteger) ν 's in Refs. [46], and applied in various contexts in Refs. [62].

Since for each given N_f we have a specific underlying pQCD running coupling $a(Q^2; N_f)$ in Eq. (45), we have then the corresponding MPT_{N_f} model. In general, m_{gl} may depend on N_f , as does the scale $\bar{\Lambda}_{N_f}$.

The generalized logarithmic derivatives $\tilde{\mathcal{A}}_\nu$ are evaluated by Eq. (24) for $0 \leq \nu < 5$, i.e., with $\nu = n + 1 + \delta$ where $n + 1 = 0, 1, 2, 3, 4$ and $0 \leq \delta < 1$. We have N -loop MPT_{N_f} ($N = 1, 2, 3, 4$). We call the model 1-loop MPT_{N_f} when $a(Q^2; N_f)$ is 1-loop Eq. (4) and in the construction of \mathcal{A}_ν in Eq. (28) the right-hand side has only one term: $\mathcal{A}_\nu = \tilde{\mathcal{A}}_\nu$. We call the model 2-loop MPT_{N_f} when $a(Q^2; N_f)$ is 2-loop Eq. (11) and in the construction of \mathcal{A}_ν in Eq. (28) the right-hand side has two terms: $\mathcal{A}_\nu = \tilde{\mathcal{A}}_\nu + \tilde{k}_1(\nu)\tilde{\mathcal{A}}_{\nu+1}$ (except when $4 \leq \nu < 5$, in which case we take $\mathcal{A}_\nu = \tilde{\mathcal{A}}_\nu$). The model is called 3-loop MPT_{N_f} when $a(Q^2; N_f)$ is given by Eq. (14) with $c_2 = \bar{c}_2(N_f)$ $\overline{\text{MS}}$ value and in Eq. (28) the right-hand side has three terms: $\tilde{\mathcal{A}}_\nu = \tilde{\mathcal{A}}_\nu + \tilde{k}_1(\nu)\tilde{\mathcal{A}}_{\nu+1} + \tilde{k}_2(\nu)\tilde{\mathcal{A}}_{\nu+2}$ (only two terms when $3 \leq \nu < 4$; only one term when $4 \leq \nu < 5$). The model is called 4-loop MPT_{N_f} when $a(Q^2; N_f)$ is given by the expansion (6) with $c_2 = \bar{c}_2(N_f)$ and $c_3 = \bar{c}_3(N_f)$ (and $c_j = 0$ for $j \geq 4$; $\mathcal{N} = 8$ is used) and in Eq. (28) the right-hand side has in general four terms: $\tilde{\mathcal{A}}_\nu = \tilde{\mathcal{A}}_\nu + \sum_{m=1}^3 \tilde{k}_m(\nu)\tilde{\mathcal{A}}_{\nu+m}$ (only three terms when $2 \leq \nu < 3$; etc.).

If we take specific (input) values of the dynamical masses $m_{\text{gl}}(N_f)$ (for $N_f = 3, 4, 5, 6$), and a specific value of $\bar{\Lambda}_3$, the values of other scales $\bar{\Lambda}_{N_f}$ (for $N_f = 4, 5, 6$) can be obtained by applying the quark threshold relations (16) written within MPT model

$$\begin{aligned} \mathcal{A}'_1 &= \mathcal{A}_1 - \mathcal{A}_2 \frac{\ell_h}{6} + \mathcal{A}_3 \left(\frac{\ell_h^2}{36} - \frac{19}{24} \ell_h + \tilde{c}_2 \right) + \mathcal{A}_4 \left[-\frac{\ell_h^3}{216} \right. \\ &\quad \left. - \frac{131}{576} \ell_h^2 + \frac{\ell_h}{1728} (-6793 + 281(N_f - 1)) + \tilde{c}_3 \right], \end{aligned} \quad (48)$$

where $\mathcal{A}'_1 \equiv \mathcal{A}_1^{(\text{MPT})}(\mu_{N_f}^2; N_f - 1)$ and $\mathcal{A}_n \equiv \mathcal{A}_n^{(\text{MPT})}(\mu_{N_f}^2; N_f)$.

3.5. Examples of various couplings as a function of positive Q^2

In Figs. 6 we show the running of $\mathcal{A}_1(Q^2)$ for $Q^2 > 0$ and $N_f = 3$ for three analytic models: FAPT, $2\delta\text{anQCD}$, and MPT (with the choice $m_{\text{gl}}^2 = 0.7 \text{ GeV}^2$). For comparison, we show also the underlying pQCD coupling $a(Q^2)$, i.e., $a(Q^2)$ in the same renormalization scheme and with the same Lambert scale Λ . At low Q^2 , the divergent behavior of $a(Q^2)$ is evident, due to the Landau singularities. We observe that at $Q^2 \gtrsim 1 \text{ GeV}^2$ $2\delta\text{anQCD}$ coupling is indistinguishable from the underlying pQCD coupling, cf. also Eq. (42). FAPT and MPT anQCD couplings (presented here in 4-loop $\overline{\text{MS}}$ scheme) are more suppressed in the infrared than $2\delta\text{anQCD}$. Figs. 7 represent the couplings at $\nu = 0.3$ (and $N_f = 3$), i.e.,

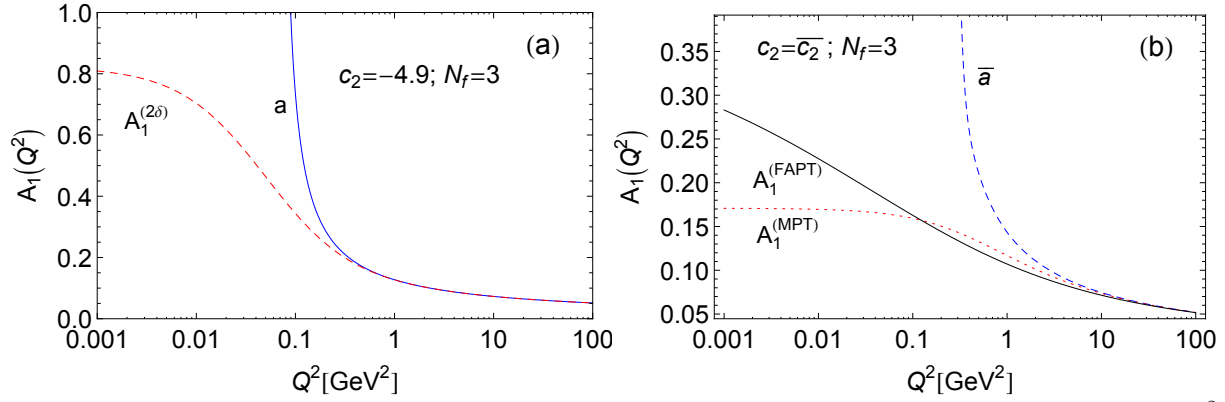


Figure 6: The couplings $\mathcal{A}_1 \equiv \mathcal{A}$ in three anQCD models with $\nu = 1$ and $N_f = 3$ as a function of Q^2 (for $Q^2 > 0$): (a) $2\delta\text{anQCD}$ coupling and pQCD coupling, in the renormalization scheme with $c_2 = -4.9$ (and $c_j = c_2^{j-1}/c_1^{j-2}$ for $j \geq 3$); the underlying pQCD coupling a is included for comparison; (b) FAPT and MPT in 4-loop $\overline{\text{MS}}$ scheme and with $\bar{\Lambda}_3^2 = 0.1 \text{ GeV}^2$; MPT with $m_{\text{gl}}^2 = 0.7 \text{ GeV}^2$; \bar{a} is a in $\overline{\text{MS}}$.

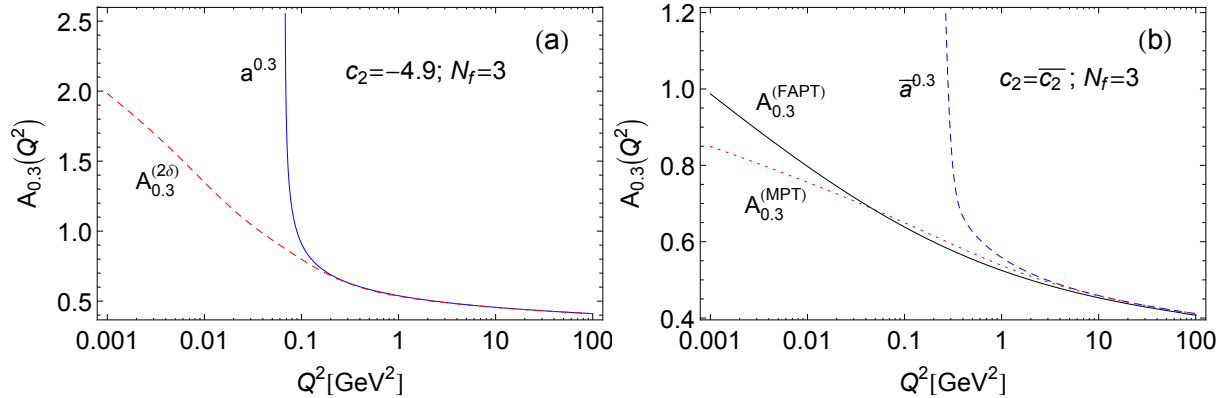


Figure 7: The same as in Figs. 6, but now with $\nu = 0.3$ ($\mathcal{A}_{\nu=0.3}$). The coupling $\mathcal{A}_{0.3}$ is calculated from the couplings $\tilde{\mathcal{A}}_{0.3+m}$ using the relation (28) (with $\nu_0 = 0.3$ and $n = 0$) with the truncation index $N = 5$ for $2\delta\text{anQCD}$ and $N = 4$ for MPT; and for FAPT using Eq. (32).

$\mathcal{A}_{\nu=0.3}(Q^2)$. We note the same behavior as in Figs. 6, but now MPT coupling increases more quickly when Q^2 decreases than in the $\nu = 1$ case.

4. Practical aspects of the program

4.1. Lambda scales and the treatment of quark thresholds

We mention some practical aspects of the program, concerning the $\bar{\Lambda}_{N_f}$ scales and the treatment of quark thresholds. The input parameter in the program is $\bar{\Lambda}_{N_f}^2$ (in GeV^2) for fixed- N_f FAPT and MPT models and $\bar{\Lambda}_3^2$ for global FAPT.¹⁴ In (fixed- N_f) $2\delta\text{anQCD}$ models, the scales $\bar{\Lambda}_{N_f}$ ($\Leftrightarrow \Lambda_{N_f}$ Lambert scales) are fixed by the world average value $a(M_Z^2; \overline{\text{MS}}; N_f = 5) = 0.1184/\pi$ [57]. In addition, the scheme parameter c_2 ($\equiv \beta_2/\beta_0$) in $2\delta\text{anQCD}_{N_f=3}$ can be adjusted by hand and can vary in the interval $-5.6 < c_2 < -2$ (see later). The quark threshold parameter is fixed to $\kappa = 2$ in the program for $2\delta\text{anQCD}$ ($\kappa_{2d}=2$), and also in FAPT ($\kappa_{\text{app}}=2$). On the other hand, in MPT, at a given N_f , there is no κ appearing, the scale $\bar{\Lambda}_{N_f}$ is an input parameter. However, the value of κ in global FAPT can be adjusted by hand in the program,¹⁵ while in $2\delta\text{anQCD}$ it should remain unchanged by construction ($\kappa_{2d}=2$). If N is the number of loops in the RGE running ($N = 1, 2, 3$ or 4), the input will be $\bar{\Lambda}_3^2 = \text{L2N1nf3}$ in global FAPT, and other scales (for other $N_f \equiv Nf$) are then given by the following functions: $\bar{\Lambda}_{N_f}^2 = \text{L2N1}[Nf, \text{L2N1nf3}]$ with $Nf = 4, 5, 6$ which is obtained via the $(N-1)$ -loop matching condition, i.e., the relation (16) where, on the right-hand side, the last included term is $\sim a^N$.

Now, we consider an example of our pQCD running coupling and their value of Lambda QCD parameter, where the perturbative N -loop running coupling for N_f is given by functions $(a1l, a2l, a3l, a4l)$, where

$$aNl[Nf, Q2, L2, \phi] \equiv a(Q^2 = Q2 \times e^{i\phi}; N_f = Nf; L2 = \bar{\Lambda}_{N_f}^2; N\text{-loop}; \overline{\text{MS}}), \quad (49)$$

where $Q2 = |Q^2|$, and $-\pi < \phi < \pi$. The global running perturbative QCD coupling is

$$aNl\text{glob}[Nf, Q2, L23, \phi] \equiv a^{(\text{glob.})}(Q^2 = Q2 \times e^{i\phi}; L23 = \bar{\Lambda}_3^2; N\text{-loop}; \overline{\text{MS}}). \quad (50)$$

Our `Mathematica` package is called by the command

¹⁴ In global FAPT, the other $\bar{\Lambda}_{N_f}$ ($N_f > 3$) are fixed from $\bar{\Lambda}_3$ by using for $a(Q^2)$ only the expansion Eq. (6) with $\mathcal{N} = 8$ (and not the RGE-numerically obtained “exact” values). But the effect of this additional approximation in comparison to Table 1 in Sec. 2.2 is small. For example, for $\bar{\Lambda}_3 = 341.8$ MeV case with 4/3-loop approach and $\kappa = 2$ (the first line in Table 1), the resulting $\bar{\Lambda}_{N_f}$ becomes 296.5 MeV, 212.8 MeV, 90.3 MeV for $N_f = 4, 5, 6$, respectively, i.e., by about 0.5 MeV lower than in Table 1. In 2/1-loop approach with $\kappa = 2$, for $\bar{\Lambda}_3 = 375.3$ MeV value (i.e., the second line of Table 1), the values of $\bar{\Lambda}_{N_f}$ in this approach are 311.9 MeV, 215.8 MeV and 89.4 MeV for $N_f = 4, 5, 6$, respectively, i.e., lower than in Table 1 by less than 1 MeV.

¹⁵Physically, $1 \leq \kappa \leq 3$ appears to be a reasonable interval of possible values. The values of various $\bar{\Lambda}_{N_f}$ change very little when κ is varied.

In[1] := <<anQCD.m

Comment: We defined the physical parameters (mc= \overline{m}_c , etc.) inside of the NumDefanQCD function:

In[2] := {mc/.NumDefanQCD, mb/.NumDefanQCD, mt/.NumDefanQCD, MZ/.NumDefanQCD}
 Out[2] := {1.27, 4.2, 163., 91.1876}

Comment: Lambda squared QCD parameter $\overline{\Lambda}_5^2$ can be fixed by the value $a(M_Z^2; \overline{MS}) = 0.1184/\pi$

In[3] := L2nf5=L25/.FindRoot[a41[5,91.1876^2/L25,0] == 0.1184/Pi,{L25,0.1}]
 Out[3] := 0.0455164

4.2. Main procedures in analytic QCD models

We present here general rules on how to use the anQCD.m package. For more detailed description we refer to Appendix A. We present the main functions that we provide to the community:

- $\text{trNl}[N_f, \nu, k, \sigma, \overline{\Lambda}_{N_f}^2]$ returns the N -loop perturbative spectral density $\rho_{\nu,k}^{(N)}(\sigma; N_f) = \text{Im} [a^\nu \ln^k a]_{Q^2=-\sigma-i\epsilon}$ ($N = 1, 2, 3, 4$) of real power ν and logarithmic power k at σ and at fixed number of active quark flavors N_f :

$$\text{trNl}[N_f, \nu, k, \sigma, L2] = \rho_{\nu,k}^{(N)}[\sigma; N_f = N_f; L2 = \overline{\Lambda}_{N_f}^2] \quad (51)$$

$(\nu \in \mathcal{R}; k = 0, 1, \dots; N = 1, 2, 3, 4; N_f = 3, 4, 5, 6).$

- $\text{trNlglob}[\nu, k, \sigma, \overline{\Lambda}_3^2]$ returns the N -loop global perturbative spectral density $\rho_{\nu,k}^{(N)\text{glob.}}(\sigma; N_f)$ ($N = 1, 2, 3, 4$) of real power ν and logarithmic power k at σ , and with $\overline{\Lambda}_3$ being the QCD $N_f = 3$ scale:

$$\text{trNlglob}[\nu, k, \sigma, L23] = \rho_{\nu,k}^{(N)\text{glob.}}[\sigma; L23 = \overline{\Lambda}_3^2], \quad (N = 1, 2, 3, 4). \quad (52)$$

- $\text{AFAPTn1}[N_f, \nu, k, |Q^2|, \Lambda^2, \phi]$ returns the N -loop ($N = 1, 2, 3, 4$) analytic FAPT coupling $\mathcal{A}_{\nu,k}^{(\text{FAPT}, N)}(Q^2, N_f) = (a^\nu(Q^2) \ln^k a(Q^2))_{\text{an.FAPT}}$, of real power ν and logarithmic power k at fixed number of active quark flavors N_f , in the Euclidean domain $[Q^2 = |Q^2| \exp(i\phi) \in \mathcal{C}$ and $Q^2 \not\leq 0]$, with Q^2 in units of GeV^2 and ϕ in radians

$$\begin{aligned} & \text{AFAPTn1}[N_f, \nu, k, Q2, L2, \phi] = \\ & = \mathcal{A}_{\nu,k}^{(\text{FAPT}, N)}[Q2 = |Q^2|, \phi = \arg(Q^2); N_f = N_f; L2 = \overline{\Lambda}_{N_f}^2] \\ & \quad (N = 1, 2, 3, 4; N_f = 3, 4, 5, 6). \end{aligned} \quad (53)$$

- In the global FAPT case $\text{AFAPT}N1\text{glob}[\nu, k, |Q^2|, \Lambda_3^2, \phi]$ returns the N -loop analytic FAPT coupling $\mathcal{A}_{\nu, k}^{(\text{FAPT}, N)\text{glob.}}(Q^2)$. of real power ν and logarithmic power k , in the Euclidean domain,

$$\text{AFAPT}N1\text{glob}[\nu, k, Q2, L23, \phi] = \mathcal{A}_{\nu, k}^{(\text{FAPT}, N)\text{glob.}}[Q2 = |Q^2|, \phi = \arg(Q^2); L23 = \bar{\Lambda}_3^2] \\ (N = 1, 2, 3, 4). \quad (54)$$

- $\text{tA2d}[N_f, \nu, |Q^2|, \phi]$ returns the analytic $2\delta\text{anQCD}$ coupling $\tilde{\mathcal{A}}_\nu^{(2\delta)}(Q^2, N_f)$, the generalized logarithmic derivative with index ν ($\nu > -1$ and real, in general non-integer), at fixed number of active quark flavors N_f , in the Euclidean domain $Q^2 = |Q^2| \exp(i\phi) \in \mathcal{C} \setminus [-M_{\text{thr.}}^2, -\infty)$ where $M_{\text{thr.}}^2 = M_2^2$ ($= s2s0[N_f]LL2[N_f]$)

$$\text{tA2d}[N_f, \nu, Q2, \phi] = \tilde{\mathcal{A}}_\nu^{(2\delta)}[Q2 = |Q^2|, \phi = \arg(Q^2); N_f = N_f], \\ (N_f = 3, 4, 5, 6; \nu > -1). \quad (55)$$

- $\text{A2d}N1[N_f, n, \nu, |Q^2|, \phi]$ returns the N -loop analytic $2\delta\text{anQCD}$ coupling $\mathcal{A}_{n+\nu}^{(2\delta)}(Q^2, N_f)$, of fractional power $n + \nu$ ($\nu > -1$ and real; $n = 0, 1, \dots, N - 1$) at fixed number of active quark flavors N_f , in the Euclidean domain $Q^2 = |Q^2| \exp(i\phi) \in \mathcal{C} \setminus [-M_{\text{thr.}}^2, -\infty)$ where $M_{\text{thr.}}^2 = M_2^2$, used for the $N^{N-1}\text{LO}$ truncation approach [cf. Eqs. (26)-(30), in particular Eq. (28) with $\nu \mapsto \nu_0$]

$$\text{A2d}N1[N_f, n, \nu, Q2, \phi] = \mathcal{A}_{\nu+n}^{(2\delta)}[Q2 = |Q^2|, \phi = \arg(Q^2); N_f = N_f], \\ (N = 1, 2, 3, 4, 5; N_f = 3, 4, 5, 6; n = 0, 1, \dots, N - 1). \quad (56)$$

- $\text{tAMPT}N1[N_f, n, \nu, Q^2, m_{\text{gl}}^2, \bar{\Lambda}_{N_f}^2]$ returns the N -loop ($N = 1, 2, 3, 4$) analytic MPT coupling $\tilde{\mathcal{A}}_{n+\nu}^{(\text{MPT}, N)}(Q^2, m_{\text{gl}}^2, N_f)$, the generalized logarithmic derivative with index $n + \nu$ ($n = 0, 1, 2, 3, 4; 0 \leq \nu < 1$), at fixed number of active quark flavors N_f , with Q^2 in the Euclidean domain ($Q^2 \in \mathcal{C}$ and $Q^2 \not\prec 0$)

$$\text{tAMPT}N1[N_f, n, \nu, Q2, M2, L2] = \\ = \tilde{\mathcal{A}}_{n+\nu}^{(\text{MPT}, N)}[Q2 = Q^2 \in \mathcal{C}; N_f = N_f; M2 = m_{\text{gl}}^2; L2 = \bar{\Lambda}_{N_f}^2] \\ (N = 1, 2, 3, 4; N_f = 3, 4, 5, 6); n = 0, 1, 2, 3, 4; 0 \leq \nu < 1). \quad (57)$$

- $\text{AMPT}N1[N_f, \nu, Q^2, m_{\text{gl}}^2, \bar{\Lambda}_{N_f}^2]$ returns the N -loop ($N = 1, 2, 3, 4$) analytic MPT coupling $\mathcal{A}_\nu^{(\text{MPT}, N)}(Q^2, m_{\text{gl}}^2, N_f)$, of fractional power ν ($0 < \nu < 5$) and at fixed number of active quark flavors N_f , with Q^2 in the Euclidean domain ($Q^2 \in \mathcal{C}$ and $Q^2 \not\prec 0$)

$$\text{AMPT}N1[N_f, \nu, Q2, M2, L2] = \\ = \mathcal{A}_\nu^{(\text{MPT}, N)}[Q2 = Q^2 \in \mathcal{C}; N_f = N_f; M2 = m_{\text{gl}}^2; L2 = \bar{\Lambda}_{N_f}^2] \\ (N = 1, 2, 3, 4; N_f = 3, 4, 5, 6); 0 < \nu < 5). \quad (58)$$

4.3. Examples of the use

With the main procedures and definitions given above, we provide a few examples of the use of these quantities for **Mathematica** 9.0.1 and **Mathematica** 10.0.1.

```
In[1] := <<anQCD.m;
```

We illustrate now how to obtain the values of the analytic couplings at what we call the three-loop level ($N = 3$), i.e., the underlying pQCD coupling is given by Eq. (14) with $c_2 = c_2(N_f; \overline{\text{MS}})$ in FAPT and MPT, and $c_2 = -4.9$ in $2\delta\text{anQCD}$. Thus, we evaluate $\mathcal{A}_{\nu,0}^{(\text{FAPT},N)}(Q^2)$, $\mathcal{A}_{\nu,0}^{(\text{FAPT},N)\text{glob.}}(Q^2)$, $\tilde{\mathcal{A}}_{\nu}^{(2\delta)}(Q^2)$, $\mathcal{A}_{n+\nu}^{(2\delta)}(Q^2)$, $\tilde{\mathcal{A}}_{n+\nu}^{(\text{MPT},N)}(Q^2)$ and $\mathcal{A}_{\nu}^{(\text{MPT},N)}(Q^2)$, taking the parameters: $\bar{\Lambda}_3^2 = 0.1 \text{ GeV}^2$ (in FAPT and MPT); $m_{\text{gl}}^2 = 0.7 \text{ GeV}^2$ in MPT. For the momentum scales we take $Q^2 = 10^{-3} \text{ GeV}^2$ (and $N_f = 3$); $Q^2 = 10^2 \text{ GeV}^2$ (and $N_f = 5$); $Q^2 = 0.5 \times \exp(i0.9) \text{ GeV}^2$ (and $N_f = 3$). We employ the indices $\nu = 1$; $\nu = 1.4$ ($n = 1$ and $\nu = 0.4$). The calculated values of the couplings are given below (as the *second* entry), with the corresponding typical calculation time in seconds (as the first entry, varies with various computers):¹⁶

```
In[2] := AFAPT3l[3, 1, 0, 10^-3, 0.1, 0] // Timing
Out[2] = {0.404938, 0.28312}
```

```
In[3] := AFAPT3lglob[1, 0, 10^-3, 0.1, 0] // Timing
Out[3] = {0.822874, 0.287775}
```

```
In[4] := A2d3l[3, 0, 1, 10^-3, 0] // Timing
Out[4] = {0.386942, 0.809041}
```

```
In[5] := AMPT3l[3, 1, 10^-3, 0.7, 0.1] // Timing
Out[5] = {0.150978, 0.171356}
```

```
In[6] := AFAPT3l[5, 1, 0, 10^2, 0.1, 0] // Timing
Out[6] = {0.410938, 0.0624843}
```

```
In[7] := AFAPT3lglob[1, 0, 10^2, 0.1, 0] // Timing
Out[7] = {0.809877, 0.0559854}
```

```
In[8] := A2d3l[5, 0, 1, 10^2, 0] // Timing
Out[8] = {0.510922, 0.0559197}
```

```
In[9] := AMPT3l[5, 1, 10^2, 0.7, 0.1] // Timing
Out[9] = {0.115982, 0.0627726}
```

¹⁶ The typical times are given when **Mathematica** 9.0.1 is used. When **Mathematica** 10.0.1 is used, the times are in general longer by about 20-50%.

```

In[10]:= AFAPT3l[3, 1.4, 0, 0.5, 0.1, 0.9] // Timing
Out[10]= {0.400939, 0.0458667 - 0.00873018 I}

In[11]:= AFAPT3lglob[1.4, 0, 0.5, 0.1, 0.9] // Timing
Out[11]= {0.861869, 0.0480877 - 0.00873811 I}

In[12]:= tA2d[3, 1.4, 0.5, 0.9] // Timing
Out[12]= {0.763884, 0.0694758 - 0.0380018 I}

In[13]:= A2d3l[3, 1, 0.4, 0.5, 0.9] // Timing
Out[13]= {1.543767, 0.062836 - 0.0325823 I}

In[14]:= tAMPT3l[3, 1, 0.4, 0.5 Exp[I 0.9], 0.7, 0.1] // Timing
Out[14]= {0.049993, 0.0555028 - 0.00617486 I}

In[15]:= AMPT3l[3, 1.4, 0.5 Exp[I 0.9], 0.7, 0.1] // Timing
Out[15]= {0.175973, 0.0537096 - 0.00719995 I}

```

In order to make plots of the analytic running couplings as in Fig. 6 and 7, users could construct an interpolation in order to reduce the time of calculation.

Acknowledgments This work was supported by FONDECYT (Chile) Grant No. 1130599 and DGIP (UTFSM) internal project USM No. 11.13.12 (C.A and G.C).

Appendix A. Description of the main procedures

The main functions found in our package are presented and described in the following.

- `trNl[Nf,Nu,k,sig,L2]`:

general: it computes the N -loop spectral density including possibly powers of the logarithmic coupling, $\rho_{\nu,k}^{(N)}(\sigma, N_f) = \text{Im}[a(Q^2)^\nu \ln^k(a(Q^2))]_{Q^2=-\sigma-i\epsilon}$;

input: the number of active flavors $\text{Nf}=N_f$; the power index $\text{Nu}=\nu$ and the logarithmic power index $\mathbf{k}=k$; the squared momentum argument $\text{sig}=\sigma$; the squared $\overline{\text{MS}}$ Lambda QCD parameter $\text{L2}=\overline{\Lambda}_{N_f}^2$ (all scales in GeV^2);

output: $\rho_{\nu,k}^{(N)}$;

example: In order to compute the value of the three-loop spectral density, at $\sigma = 1.5 \text{ GeV}^2$ and $N_f = 3$, and with $\overline{\Lambda}_{N_f}^2 = 0.1 \text{ GeV}^2$, i.e., the quantity $\rho_{0.5,0}^{(3)}(1.5, 3) = 0.104393$, one has to use the command `tr3l[3,0.5,0,1.5,0.1]`.

- `trNlglob[Nu,k,sig,L2nf3]`:

general: it computes the N -loop global spectral density incorporating the powers of the logarithmic coupling

$$\rho_{\nu,k}^{(N)\text{glob.}}(\sigma, N_f) = \text{Im}[a^{(\text{glob.})}(Q^2)^\nu \ln^k(a^{(\text{glob.})}(Q^2))]_{Q^2=-\sigma-i\epsilon};$$

input: the power index $\text{Nu}=\nu$ and the logarithmic power index $\mathbf{k}=k$; the squared momentum argument $\text{sig}=\sigma$; the squared $\overline{\text{MS}}$ Lambda QCD parameter at $N_f = 3$ (at the corresponding N -loop) $\text{L2nf3}=\overline{\Lambda}_3^2$ (all scales are in GeV^2);

output: $\rho_{\nu,k}^{(N)\text{glob.}}$;

example: In order to compute the value of the three-loop global spectral density at $\sigma = 1.5 \text{ GeV}^2$ and with $\overline{\Lambda}_3^2 = 0.1 \text{ GeV}^2$, i.e., the quantity

$$\rho_{0.5,0}^{(3)\text{glob.}}(1.5, 3) = 0.104393, \text{ one has to use the command } \text{tr3lglob}[0.5, 0, 1.5, 0.1].$$

- `AFAPTn1[Nf,Nu,k,Q2,L2,Fi]`:

general: it computes the N -loop coupling in FAPT_{N_f} incorporating the analytization of powers of the logarithmic coupling

$$\mathcal{A}_{\nu,k}^{(\text{FAPT},N)}(Q^2, N_f) = (a^\nu(Q^2) \ln^k a(Q^2))_{\text{an.FAPT}} \text{ in the Euclidean domain};$$

input: the number of active flavors $\text{Nf}=N_f$; the power index $\text{Nu}=\nu$ and the logarithmic power index $\mathbf{k}=k$; the squared momentum argument $\text{Q2}=|Q^2|$; the squared $\overline{\text{MS}}$ Lambda QCD parameter $\text{L2}=\overline{\Lambda}_{N_f}^2$; the phase of the complex $Q^2 = |Q^2|e^{i\phi}$, i.e., $\text{Fi}=\phi$ (in radians); all scales are in GeV^2 ;

output: $\mathcal{A}_{\nu,k}^{(\text{FAPT},N)}$;

example: In order to compute the value of the three-loop FAPT coupling \mathcal{A}_ν at $Q^2 = 1.5 \text{ GeV}^2$, with $\nu = 0.5$, $N_f = 3$ and $\overline{\Lambda}_3^2 = 0.1 \text{ GeV}^2$, i.e., the quantity

$$\mathcal{A}_{0.5,0}^{(\text{FAPT},3)}(1.5, 3) = 0.324597, \text{ one has to use the command } \text{AFAPT31}[3, 0.5, 0, 1.5, 0.1, 0].$$

- `AFAPTnlglob[Nu,k,Q2,L2nf3,Fi]`:

general: it computes the N -loop global FAPT coupling $\mathcal{A}_{\nu,k}^{(\text{FAPT},N)\text{glob.}}(Q^2)$ in the Euclidean domain;

input: the power index $\text{Nu}=\nu$ and the logarithmic power index $\mathbf{k}=k$; the squared momentum argument $\text{Q2}=|Q^2|$; the squared $\overline{\text{MS}}$ Lambda QCD parameter at $N_f = 3$ $\text{L2nf3}=\overline{\Lambda}_3^2$; the phase of the complex $Q^2 = |Q^2|e^{i\phi}$, i.e., $\text{Fi}=\phi$ (in radians); all scales are in GeV^2 ;

output: $\mathcal{A}_{\nu,k}^{(\text{FAPT},N)\text{glob.}}$;

example: In order to compute the value of the three-loop FAPT coupling \mathcal{A}_ν at $Q^2 = 1.5 \text{ GeV}^2$, with $\nu = 0.5$ and $\overline{\Lambda}_3^2 = 0.1 \text{ GeV}^2$, i.e., the quantity

$\mathcal{A}_{0.5,0}^{(\text{FAPT},3)\text{glob.}}$ (1.5) = 0.333458, one has to use the command
`AFAPT31glob[0.5, 0, 1.5, 0.1, 0]`.

- `tA2d[Nf,nu,Q2,Fi]`:

general: it computes coupling $\tilde{\mathcal{A}}_{\text{nu}}^{(2\delta)}(Q^2, N_f)$ in $2\delta\text{anQCD}_{N_f}$, the generalized logarithmic derivative with index `nu`, in the Euclidean domain;

input: the number of active flavors `Nf`= N_f ; the index $\nu = \text{nu}$ (`nu` > -1 and real); the squared momentum argument `Q2`= $|Q^2|$ (in GeV^2); `Fi`= ϕ is the phase of the complex $Q^2 = |Q^2|e^{i\phi}$ (in radians);

output: $\tilde{\mathcal{A}}_{\nu}^{(2\delta,N)}$;

example: In order to compute the value of $\tilde{\mathcal{A}}_{\nu}$ at $Q^2 = 0.5 \text{ GeV}^2$, with `nu` = 1.4, and $N_f = 3$, i.e., the coupling $\tilde{\mathcal{A}}_{1.4}^{(2\delta,3)}(0.5) = 0.0827052$, one has to use the command `tA2d[3, 1.4, 0.5, 0]`.

- `A2dN1[Nf,n,nu,Q2,Fi]`:

general: it computes N -loop coupling $\mathcal{A}_{\text{nu}+n}^{(2\delta)}(Q^2, N_f)$ in $2\delta\text{anQCD}_{N_f}$ in the Euclidean domain;

input: the number of active flavors `Nf`= N_f ; the indices `n` (`n` is nonnegative integer) and `nu` (`nu` > -1 and real); the squared momentum argument `Q2`= $|Q^2|$ (in GeV^2), `Fi`= ϕ is the phase of the complex $Q^2 = |Q^2|e^{i\phi}$ (in radians); see also Eq. (28), with $\nu_0 \mapsto \text{nu}$ and $n \mapsto \text{n}$;

output: $\mathcal{A}_{\nu+n}^{(2\delta,N)}$;

example: In order to compute the value of the “three-loop” 2danQCD coupling \mathcal{A}_{ν} at $Q^2 = 0.5 \text{ GeV}^2$, with `nu` = 0.4, `n` = 1 and $N_f = 3$, i.e., the coupling $\mathcal{A}_{1.4}^{(2\delta,3)}(0.5) = 0.0745576$, one has to use the command `A2d31[3, 1, 0.4, 0.5, 0]`.

- `tAMPTN1[Nf,n,nu,Q2,M2,L2MPT]`:

general: it computes the coupling $\tilde{\mathcal{A}}_{\text{n}+\text{nu}}^{(\text{MPT},N)}(Q^2, m_{\text{gl}}^2, N_f)$, the generalized logarithmic derivative with index `n` + `nu`, in MPT_{N_f} in the Euclidean domain;

input: the number of active flavors `Nf` = N_f ; the integer index `n` (`n` = 0, 1, 2, 3, 4) and the noninteger index `nu`= ν ($0 \leq \nu < 1$); the squared momentum argument `Q2`= Q^2 (complex in general); the effective mass parameter `M2`= m_{gl}^2 ; the squared $\overline{\text{MS}}$ Lambda QCD parameter `L2MPT`= $\overline{\Lambda}_{N_f}^2$ (all scales in GeV^2); all scales are in GeV^2 ;

output: $\tilde{\mathcal{A}}_{\text{n}+\nu}^{(\text{MPT},N)}$;

example: In order to compute the value of the three-loop MPT coupling $\tilde{\mathcal{A}}_{\text{n}+\nu}$ with $N_f = 3$, with `n` = 1 and $\nu = 0.4$, at $Q^2 = 0.5 \text{ GeV}^2$, with $m_{\text{gl}}^2 = 0.7 \text{ GeV}^2$, and

$\bar{\Lambda}_3^2 = 0.1 \text{ GeV}^2$, i.e., the quantity $\tilde{\mathcal{A}}_{1.4}^{(\text{MPT},3)}(0.5, 0.7, 3) = 0.0528178$, one has to use the command `tAMPT31 [3, 1, 0.4, 0.5, 0.7, 0.1]`.

- `AMPTN1 [Nf, Nu, Q2, M2, L2MPT]`:

general: it computes the N -loop coupling $\mathcal{A}_\nu^{(\text{MPT},N)}(Q^2, m_{\text{gl}}^2, N_f)$ in MPT_{N_f} in the Euclidean domain;

input: the number of active flavors $\text{Nf}=N_f$; the index $\text{Nu}=\nu$ ($0 < \nu < 5$); the squared momentum argument $\text{Q2}=Q^2$ (complex in general); the squared $\overline{\text{MS}}$ Lambda QCD parameter $\text{L2MPT}=\bar{\Lambda}_{N_f}^2$; the effective mass parameter $\text{M2}=m_{\text{gl}}^2$ (all scales in GeV^2);

output: $\mathcal{A}_\nu^{(\text{MPT},N)}$;

example: In order to compute the value of the three-loop MPT coupling \mathcal{A}_ν with $N_f = 3$, $\nu = 1.4$, at $Q^2 = 0.5 \text{ GeV}^2$, with $m_{\text{gl}}^2 = 0.7 \text{ GeV}^2$, and $\bar{\Lambda}_3^2 = 0.1 \text{ GeV}^2$, i.e., the quantity $\mathcal{A}_{1.4}^{(\text{MPT},3)}(0.5, 0.7, 3) = 0.0514469$, one has to use the command `AMPT31 [3, 1.4, 0.5, 0.7, 0.1]`.

All scales $\bar{\Lambda}_{N_f}^2$, Q^2 (Euclidean), and spectral-integration variables σ are in GeV^2 . The number of loops N is specified in the names of the procedures, except in `2delta_nQCD` where the underlying pQCD coupling is given by Eq. (14) with $c_2 = -4.9$ (this value can be changed by hand in the program `anQCD.m`, by replacing “`c22din=-4.9;`” by another value, between -5.6 and -2.0).

References

- [1] N.N. Bogoliubov and D.V. Shirkov, *Introduction to the Theory of Quantum Fields*, New York, Wiley, 1959; 1980.
- [2] R. Oehme, *Analytic structure of amplitudes in gauge theories with confinement—/*, Int. J. Mod. Phys. A **10** (1995) 1995 [arXiv:hep-th/9412040].
- [3] D. Zwanziger, *Nonperturbative Faddeev-Popov formula and infrared limit of QCD*, Phys. Rev. D **69** (2004) 016002 [hep-ph/0303028]; D. Dudal, J. A. Gracey, S. P. Sorella, N. Vandersickel and H. Verschelde, *A Refinement of the Gribov-Zwanziger approach in the Landau gauge: infrared propagators in harmony with the lattice results*, Phys. Rev. D **78** (2008) 065047 [arXiv:0806.4348 [hep-th]].
- [4] L. von Smekal, R. Alkofer and A. Hauck, *The Infrared behavior of gluon and ghost propagators in Landau gauge QCD*, Phys. Rev. Lett. **79** (1997) 3591 [hep-ph/9705242]; C. Lerche and L. von Smekal, *On the infrared exponent for gluon and ghost propagation in Landau gauge QCD*, Phys. Rev. D **65** (2002) 125006 [hep-ph/0202194]; C. S. Fischer and J. M. Pawłowski, *Uniqueness of infrared asymptotics in Landau gauge Yang-Mills theory*, Phys. Rev. D **75** (2007) 025012 [hep-th/0609009]; C. S. Fischer, A. Maas and J. M. Pawłowski, *On the infrared behavior of Landau gauge Yang-Mills theory*, Annals Phys. **324** (2009) 2408 [arXiv:0810.1987 [hep-ph]].

- [5] A. C. Aguilar and J. Papavassiliou, *Power-law running of the effective gluon mass*, Eur. Phys. J. A **35** (2008) 189 [arXiv:0708.4320 [hep-ph]]; A. C. Aguilar, D. Binosi, J. Papavassiliou and J. Rodriguez-Quintero, *Non-perturbative comparison of QCD effective charges*, Phys. Rev. D **80** (2009) 085018 [arXiv:0906.2633 [hep-ph]].
- [6] D. Zwanziger, *Nonperturbative Landau gauge and infrared critical exponents in QCD*, Phys. Rev. D **65** (2002) 094039 [hep-th/0109224].
- [7] H. Gies, *Running coupling in Yang-Mills theory: a flow equation study*, Phys. Rev. D **66** (2002) 025006 [hep-th/0202207]; J. Braun and H. Gies, *Chiral phase boundary of QCD at finite temperature*, JHEP **0606** (2006) 024 [hep-ph/0602226]; J. M. Pawłowski, D. F. Litim, S. Nedelko and L. von Smekal, *Infrared behavior and fixed points in Landau gauge QCD*, Phys. Rev. Lett. **93** (2004) 152002 [hep-th/0312324].
- [8] J. C. R. Bloch, A. Cucchieri, K. Langfeld and T. Mendes, Nucl. Phys. B **687** (2004) 76 [hep-lat/0312036]; S. Furui and H. Nakajima, Phys. Rev. D **70** (2004) 094504 [hep-lat/0403021]; S. Furui, *Self-dual gauge fields, domain wall fermion zero modes and the Kugo-Ojima confinement criterion*, PoS LAT **2009** (2009) 227 [arXiv:0908.2768 [hep-lat]]; A. Sternbeck and L. von Smekal, *Infrared exponents and the strong-coupling limit in lattice Landau gauge*, Eur. Phys. J. C **68** (2010) 487 [arXiv:0811.4300 [hep-lat]].
- [9] S. J. Brodsky, G. F. de Teramond and A. Deur, *Nonperturbative QCD coupling and its β -function from Light-Front Holography*, Phys. Rev. D **81** (2010) 096010 [arXiv:1002.3948 [hep-ph]]; T. Gutsche, V. E. Lyubovitskij, I. Schmidt and A. Vega, *Dilaton in a soft-wall holographic approach to mesons and baryons*, Phys. Rev. D **85** (2012) 076003 [arXiv:1108.0346 [hep-ph]].
- [10] Yu. A. Simonov, *Perturbative theory in the nonperturbative QCD vacuum*, Phys. Atom. Nucl. **58** (1995) 107 [Yad. Fiz. **58** (1995) 113] [hep-ph/9311247]; *Asymptotic freedom and IR freezing in QCD: the role of gluon paramagnetism*, arXiv:1011.5386 [hep-ph].
- [11] A. M. Badalian and D. S. Kuzmenko, *Freezing of QCD coupling α_s affects the short distance static potential*, Phys. Rev. D **65** (2001) 016004 [hep-ph/0104097]; A. M. Badalian, *Strong coupling constant in coordinate space*, Phys. Atom. Nucl. **63** (2000) 2173 [Yad. Fiz. **63** (2000) 2269].
- [12] B. Badelek, J. Kwiecinski and A. Stasto, *A Model for F_L and $R = F_L/F_T$ at low x and low Q^2* , Z. Phys. C **74** (1997) 297 [hep-ph/9603230].
- [13] A. V. Kotikov, V. G. Krivokhizhin and B. G. Shaikhatdenov, *Analytic and 'frozen' QCD coupling constants up to NNLO from DIS data*, Phys. Atom. Nucl. **75** (2012) 507 [arXiv:1008.0545 [hep-ph]].

- [14] A. Deur, V. Burkert, J. P. Chen and W. Korsch, *Determination of the effective strong coupling constant $\alpha_{s,g1}(Q^2)$ from CLAS spin structure function data*, Phys. Lett. B **665** (2008) 349 [arXiv:0803.4119 [hep-ph]].
- [15] A. Courtoy and S. Liuti, *Extraction of α_s from deep inelastic scattering at large x* , Phys. Lett. B **726** (2013) 320 [arXiv:1302.4439 [hep-ph]].
- [16] D. V. Shirkov, I. L. Solovtsov, *Analytic QCD running coupling with finite IR behaviour and universal $\bar{\alpha}_s(0)$ value*, JINR Rapid Commun. 2[76] (1996) 5–10, [arXiv:hep-ph/9604363]. arXiv:hep-ph/9604363
Analytic model for the QCD running coupling with universal $\bar{\alpha}_s(0)$ value, Phys. Rev. Lett. **79** (1997) 1209–1212, [arXiv:hep-ph/9704333]. arXiv:hep-ph/9704333
- [17] K. A. Milton, I. L. Solovtsov, *Analytic perturbation theory in QCD and Schwinger’s connection between the beta function and the spectral density*, Phys. Rev. D **55** (1997) 5295–5298, [arXiv:hep-ph/9611438]. arXiv:hep-ph/9611438
- [18] I. L. Solovtsov, D. V. Shirkov, *Analytic approach to perturbative QCD and renormalization scheme dependence*, Phys. Lett. B **442** (1998) 344–348, [arXiv:hep-ph/9711251]. arXiv:hep-ph/9711251
- [19] D. V. Shirkov, *Analytic perturbation theory for QCD observables*, Theor. Math. Phys. **127** (2001) 409 [hep-ph/0012283]; *Analytic perturbation theory in analyzing some QCD observables*, Eur. Phys. J. C **22** (2001) 331 [hep-ph/0107282].
- [20] A. P. Bakulev, S. V. Mikhailov, N. G. Stefanis, *QCD analytic perturbation theory: from integer powers to any power of the running coupling*, Phys. Rev. D **72** (2005) 074014; Erratum: *ibid.* D **72** (2005) 119908(E), [arXiv:hep-ph/0506311]. arXiv:hep-ph/0506311
- [21] A. P. Bakulev, A. I. Karanikas and N. G. Stefanis, *Analyticity properties of three-point functions in QCD beyond leading order*, Phys. Rev. D **72** (2005) 074015 [hep-ph/0504275].
- [22] A. P. Bakulev, S. V. Mikhailov and N. G. Stefanis, *Fractional Analytic Perturbation Theory in Minkowski space and application to Higgs boson decay into a b anti- b pair*, Phys. Rev. D **75** (2007) 056005; Erratum: *ibid.* D **77** (2008) 079901(E) [hep-ph/0607040].
- [23] A. P. Bakulev, S. V. Mikhailov and N. G. Stefanis, JHEP **1006** (2010) 085 [arXiv:1004.4125 [hep-ph]].
- [24] A. V. Nesterenko, *Quark antiquark potential in the analytic approach to QCD*, Phys. Rev. D **62** (2000) 094028 [arXiv:hep-ph/9912351]; *New analytic running coupling in spacelike and timelike regions*, Phys. Rev. D **64** (2001) 116009 [arXiv:hep-ph/0102124]; *Analytic invariant charge in QCD*, Int. J. Mod. Phys. A **18** (2003)

- 5475 [arXiv:hep-ph/0308288]; A. C. Aguilar, A. V. Nesterenko and J. Papavassiliou, *Infrared enhanced analytic coupling and chiral symmetry breaking in QCD*, J. Phys. G **31** (2005) 997 [hep-ph/0504195].
- [25] A. V. Nesterenko and J. Papavassiliou, *The massive analytic invariant charge in QCD*, Phys. Rev. D **71** (2005) 016009 [hep-ph/0410406]; *Infrared behavior of the Adler function from a novel dispersion relation*, J. Phys. G **32** (2006) 1025 [arXiv:hep-ph/0511215]; A. V. Nesterenko, *Adler function in the analytic approach to QCD*, eConf C **0706044** (2007) 25 [arXiv:0710.5878 [hep-ph]].
- [26] B. R. Webber, *QCD power corrections from a simple model for the running coupling*, JHEP **9810** (1998) 012 [hep-ph/9805484].
- [27] G. Cvetič and C. Valenzuela, *An approach for evaluation of observables in analytic versions of QCD*, J. Phys. G **32** (2006) L27 [arXiv:hep-ph/0601050].
- [28] G. Cvetič and C. Valenzuela, *Various versions of analytic QCD and skeleton-motivated evaluation of observables*, Phys. Rev. D **74** (2006) 114030; Erratum: *ibid.* D **84** (2011) 019902(E) [arXiv:hep-ph/0608256].
- [29] A. I. Alekseev, *Synthetic running coupling of QCD*, Few Body Syst. **40** (2006) 57 [arXiv:hep-ph/0503242].
- [30] C. Contreras, G. Cvetič, O. Espinosa and H. E. Martínez, *Simple analytic QCD model with perturbative QCD behavior at high momenta*, Phys. Rev. D **82** (2010) 074005 [arXiv:1006.5050].
- [31] C. Ayala, C. Contreras and G. Cvetič, *Extended analytic QCD model with perturbative QCD behavior at high momenta*, Phys. Rev. D **85** (2012) 114043 [arXiv:1203.6897 [hep-ph]]; in Eqs. (21) and (22) of this reference there is a typo: the lower limit of integration is written as $s_L - \eta$; it is in fact $-s_L - \eta$.
- [32] D. V. Shirkov, *'Massive' perturbative QCD, regular in the IR limit*, Phys. Part. Nucl. Lett. **10** (2013) 186 [arXiv:1208.2103 [hep-th]].
- [33] K. A. Milton, I. L. Solovtsov and O. P. Solovtsova, *Analytic perturbation theory and inclusive tau decay*, Phys. Lett. B **415** (1997) 104 [arXiv:hep-ph/9706409]; *The Adler function for light quarks in analytic perturbation theory*, Phys. Rev. D **64** (2001) 016005 [arXiv:hep-ph/0102254];
- [34] B. A. Magradze, *The gluon propagator in analytic perturbation theory*, Conf. Proc. C **980518** (1999) 158 [hep-ph/9808247].
- [35] M. Baldicchi, A. V. Nesterenko, G. M. Prosperi, D. V. Shirkov and C. Simolo, *Bound state approach to the QCD coupling at low energy scales*, Phys. Rev. Lett. **99** (2007) 242001 [arXiv:0705.0329 [hep-ph]]; M. Baldicchi, A. V. Nesterenko, G. M. Prosperi

- and C. Simolo, *QCD coupling below 1 GeV from quarkonium spectrum*, Phys. Rev. D **77** (2008) 034013 [arXiv:0705.1695 [hep-ph]].
- [36] S. Peris, M. Perrottet and E. de Rafael, *Matching long and short distances in large- N_c QCD*, JHEP **9805** (1998) 011 [arXiv:hep-ph/9805442].
- [37] B. A. Magradze, *Testing the concept of quark-hadron duality with the ALEPH τ decay data*, Few Body Syst. **48** (2010) 143; Erratum: *ibid.* **53** (2012) 365(E) [arXiv:1005.2674 [hep-ph]]; *Strong coupling constant from τ decay within a dispersive approach to perturbative QCD*, Proceedings of A. Razmadze Mathematical Institute 160 (2012) 91-111 [arXiv:1112.5958 [hep-ph]].
- [38] A. V. Nesterenko, *Hadronic effects in low-energy QCD: inclusive tau lepton decay*, Nucl. Phys. Proc. Suppl. **234** (2013) 199 [arXiv:1209.0164 [hep-ph]]; *Dispersive approach to QCD and inclusive tau lepton hadronic decay*, Phys. Rev. D **88** (2013) 056009 [arXiv:1306.4970 [hep-ph]]; *Inclusive tau lepton decay: the effects due to hadronization*, PoS ConfinementX (2012) 350 [arXiv:1302.0518 [hep-ph]].
- [39] G. Cvetič and C. Villavicencio, *Operator Product Expansion with analytic QCD in tau decay physics*, Phys. Rev. D **86** (2012) 116001 [arXiv:1209.2953 [hep-ph]]; C. Ayala and G. Cvetič, *Calculation of binding energies and masses of quarkonia in analytic QCD models*, Phys. Rev. D **87** (2013) 5, 054008 [arXiv:1210.6117 [hep-ph]]; P. Allendes, C. Ayala and G. Cvetič, *Gluon propagator in Fractional Analytic Perturbation Theory*, Phys. Rev. D **89** (2014) 5, 054016 [arXiv:1401.1192 [hep-ph]].
- [40] G. M. Prosperi, M. Raciti and C. Simolo, *On the running coupling constant in QCD*, Prog. Part. Nucl. Phys. **58** (2007) 387 [arXiv:hep-ph/0607209].
- [41] D. V. Shirkov and I. L. Solovtsov, *Ten years of the analytic perturbation theory in QCD*, Theor. Math. Phys. **150** (2007) 132 [arXiv:hep-ph/0611229].
- [42] G. Cvetič and C. Valenzuela, *Analytic QCD: a short review*, Braz. J. Phys. **38** (2008) 371 [arXiv:0804.0872 [hep-ph]].
- [43] A. P. Bakulev, *Global Fractional Analytic Perturbation Theory in QCD with selected applications*, Phys. Part. Nucl. **40** (2009) 715 [arXiv:0805.0829 [hep-ph]] (arXiv preprint in Russian).
- [44] A. P. Bakulev and D. V. Shirkov, *Inevitability and importance of non-perturbative elements in Quantum Field Theory*, [arXiv:1102.2380 [hep-ph]].
- [45] N. G. Stefanis, *Taming Landau singularities in QCD perturbation theory: the analytic approach*, Phys. Part. Nucl. **44** (2013) 494 [arXiv:0902.4805 [hep-ph]].
- [46] G. Cvetič and A. V. Kotikov, *Analogs of noninteger powers in general analytic QCD*, J. Phys. G **39**, 065005 (2012), [arXiv:1106.4275 [hep-ph]].

- [47] A. V. Nesterenko and C. Simolo, *QCDMPT: Program package for analytic approach to QCD*, Comput. Phys. Commun. **181** (2010) 1769 [arXiv:1001.0901 [hep-ph]]; QCDMPT_F: *Fortran version of QCDMPT package*, *ibid.* **182** (2011) 2303 [arXiv:1107.1045 [hep-ph]];
- [48] A. P. Bakulev and V. L. Khandramai, *FAPT: a Mathematica package for calculations in QCD Fractional Analytic Perturbation Theory*, *ibid.* **184** (2013) 1, 183.
- [49] D. J. Gross and F. Wilczek, *Ultraviolet Behavior of Nonabelian Gauge Theories*, Phys. Rev. Lett. **30**, 1343 (1973); H. D. Politzer, *Reliable Perturbative Results for Strong Interactions?*, Phys. Rev. Lett. **30**, 1346 (1973).
- [50] W. E. Caswell, *Asymptotic Behavior of Nonabelian Gauge Theories to Two Loop Order*, Phys. Rev. Lett. **33** (1974) 244; D. R. T. Jones, *Two Loop Diagrams in Yang-Mills Theory*, Nucl. Phys. B **75** (1974) 531; E. Egorian and O. V. Tarasov, *Two Loop Renormalization of the QCD in an Arbitrary Gauge*, Teor. Mat. Fiz. **41** (1979) 26 [Theor. Math. Phys. **41** (1979) 863].
- [51] P. M. Stevenson, *Optimized Perturbation Theory*, Phys. Rev. D **23** (1981) 2916.
- [52] O. V. Tarasov, A. A. Vladimirov and A. Y. Zharkov, *The Gell-Mann-Low Function of QCD in the Three Loop Approximation*, Phys. Lett. B **93** (1980) 429; S. A. Larin and J. A. M. Vermaseren, *The Three loop QCD Beta function and anomalous dimensions*, Phys. Lett. B **303** (1993) 334 [hep-ph/9302208].
- [53] T. van Ritbergen, J. A. M. Vermaseren and S. A. Larin, *The Four loop beta function in quantum chromodynamics*, Phys. Lett. B **400** (1997) 379 [hep-ph/9701390].
- [54] D. S. Kourashev, *The QCD observables expansion over the scheme-independent two-loop coupling constant powers, the scheme dependence reduction*, arXiv:hep-ph/9912410; D. S. Kurashev and B. A. Magradze, *Explicit expressions for time-like and spacelike observables of quantum chromodynamics in analytic perturbation theory*, Teor. Math. Phys. **135** (2003) 531 [Teor. Mat. Fiz. **135** (2003) 95]; B. A. Magradze, *A novel series solution to the renormalization group equation in QCD*, Few Body Syst. **40**, 71 (2006) [hep-ph/0512374].
- [55] E. Gardi, G. Grunberg and M. Karliner, *Can the QCD running coupling have a causal analyticity structure?*, JHEP **9807** (1998) 007 [hep-ph/9806462].
- [56] K. G. Chetyrkin, B. A. Kniehl and M. Steinhauser, *Strong coupling constant with flavor thresholds at four loops in the \overline{MS} scheme*, Phys. Rev. Lett. **79** (1997) 2184 [hep-ph/9706430].
Decoupling relations to $\mathcal{O}(\alpha_s^3)$ and their connection to low-energy theorems, Nucl. Phys. B **510** (1998) 61 [hep-ph/9708255].
- [57] J. Beringer *et al.* [Particle Data Group Collaboration], *Review of Particle Physics (RPP)*, Phys. Rev. D **86** (2012) 010001.

- [58] C. Ayala, G. Cvetič and A. Pineda, *The bottom quark mass from the $\Upsilon(1S)$ system at NNNLO*, JHEP **1409** (2014) 045 [arXiv:1407.2128 [hep-ph]].
- [59] C. Contreras, G. Cvetič and P. Gaete, *Calculations of binding energies and masses of heavy quarkonia using renormalon cancellation*, Phys. Rev. D **70** (2004) 034008 [hep-ph/0311202].
- [60] *MATHEMATICA 9.0.1, Wolfram Co; MATHEMATICA 10.0.1, Wolfram Co*;
- [61] A. Erdélyi, W. Magnus, F. Oberhettinger and F. G. Tricomi, *Higher Transcendental Functions, Vol. I*, McGraw-Hill Book Company, Inc., New York-Toronto-London, 1953; note that they use for $\text{Li}_{\nu'}(z)$ the Lerch function notation: $\text{Li}_{\nu'}(z) = z \Phi(z, \nu', 1) \equiv F(z, \nu')$.
- [62] G. Cvetič, *Techniques of evaluation of QCD low-energy physical quantities with running coupling with infrared fixed point*, Phys. Rev. D **89** (2014) 036003 [arXiv:1309.1696 [hep-ph]]; *Evaluations of low-energy physical quantities in QCD with IR freezing of the coupling*, Few Body Syst. **55** (2014) 567 [arXiv:1311.7611 [hep-ph]].
- [63] A. I. Karanikas and N. G. Stefanis, *Analyticity and power corrections in hard scattering hadronic functions*, Phys. Lett. B **504** (2001) 225; Erratum: *ibid.* B **636** (2006) 330(E) [hep-ph/0101031].
- [64] G. Cvetič, R. Kögerler and C. Valenzuela, *Reconciling the analytic QCD with the ITEP operator product expansion philosophy*, Phys. Rev. D **82** (2010) 114004 [arXiv:1006.4199 [hep-ph]]; C. Contreras, G. Cvetič, R. Kögerler, P. Kröger and O. Orellana, *Perturbative QCD in acceptable schemes with holomorphic coupling*, arXiv:1405.5815 [hep-ph].
- [65] G. Cvetič and H. E. Martínez, *Rational approximations in analytic QCD*, J. Phys. G **36** (2009) 125006 [arXiv:0907.0033 [hep-ph]].
- [66] G. Cvetič and R. Kögerler, *Scale- and scheme-independent extension of Padé approximants: Bjorken polarized sum rule as an example*, Phys. Rev. D **63** (2001) 056013 [arXiv:hep-ph/0006098].
- [67] E. G. S. Luna, A. L. dos Santos and A. A. Natale, *QCD effective charge and the structure function F_2 at small- x* , Phys. Lett. B **698** (2011) 52 [arXiv:1012.4443 [hep-ph]].